NASA TECHNICAL NOTE

NASA TN D-7465

NASA TN D-7465

HOT-WIRE ANEMOMETRY IN HYPERSONIC HELIUM FLOW

by Richard D. Wagner and Leonard M. Weinstein

Langley Research Center

Hampton, Va. 23665

NATIONAL AERONAUTICS AND SPACE ADMINISTRATION • WASHINGTON, D. C. • JUNE 1974

1. Report No. NASA TN D-7465	2. Government Accession No.	3. Recipient's Catalog No.
4. Title and Subtitle HOT-WIRE ANEMOMETRY IN HYPERSONIC HELIUM FLOW		5. Report Date June 1974 6. Performing Organization Code
7. Author(s) Richard D. Wagner and Leonard M. Weinstein		8. Performing Organization Report No. L-9238
9. Performing Organization Name and Address NASA Langley Research Center Hampton, Va. 23665		10. Work Unit No. 501-06-08-01 11. Contract or Grant No.
12. Sponsoring Agency Name and Address National Aeronautics and Space Administration Washington, D.C. 20546		13. Type of Report and Period Covered Technical Note 14. Sponsoring Agency Code

15. Supplementary Notes

Appendix entitled "Developments in Equipment and Probes for Mean-Flow and Fluctuating-Flow Measurements With a Hot Wire" by Leonard M. Weinstein and John R. Nayadley, Sr.

16. Abstract

Hot-wire anemometry techniques are described that have been developed and used for hypersonic-helium-flow studies at the Langley Research Center. The short run time available dictated certain innovations in applying conventional hot-wire techniques. Some examples are given to show the application of the techniques used. Some of the modifications to conventional equipment are described, including probe modifications and probe heating controls.

17. Key Words (Suggested by Author(s))	18. Distribution Statement
Hypersonic flow Turbulence measurements Hot-wire anemometry	Unclassified – Unlimited STAR Category 12

19. Security Classif. (of this report)	20. Security Classif. (of this page)	21. No. of Pages	22. Price*
Unclassified	Unclassified	45	$3.25

*For sale by the National Technical Information Service, Springfield, Virginia 22151

HOT-WIRE ANEMOMETRY IN HYPERSONIC HELIUM FLOW

By Richard D. Wagner and Leonard M. Weinstein
Langley Research Center

SUMMARY

Hot-wire anemometry techniques are described that have been developed and used for hypersonic-helium-flow studies at the Langley Research Center. The short run time available dictated certain innovations in applying conventional hot-wire techniques. Some examples are given to show the application of the techniques used. Some of the modifications to conventional equipment are described, including probe modifications and probe heating controls.

INTRODUCTION

In the early fifties, Kovasznay, reference 1, and Morkovin, reference 2, successfully extended hot-wire anemometry techniques from low-speed flow to supersonic compressible flow. A period followed in which several classic experiments were performed that used these compressible-flow anemometry techniques. Two such experiments were the Laufer-Vrebalovich experiments (see ref. 3) on supersonic laminar boundary-layer stability and Kistler's turbulence measurements (ref. 4) in supersonic turbulent boundary layers. For sometime thereafter, the field of compressible anemometry was somewhat inactive, and attempts to extend the technique to hypersonic flow were deterred by probe fabrication problems that arose because of the extreme temperature environments of hypersonic-air wind tunnels. Only recently have attempts to make quantitative hot-wire measurements in hypersonic-air wind tunnels been successful (see ref. 5, for example).

With helium as a test medium, hypersonic flow with Mach numbers as high as 35 can be produced without heating of the supply gas to avoid condensation in the test section. Because of this benign environment, the hypersonic helium tunnel offers a unique capability wherein hypersonic turbulence may be studied using simple extensions of the methods of Kovasznay and Morkovin. However, the short running time available in the typical hypersonic helium tunnel requires some innovations in the application of hot-wire techniques. The purpose of the present report is to describe the hot-wire anemometry techniques that have been used in turbulence studies in hypersonic tunnels at the Langley Research Center (refs. 6 to 12) and to relate some of the experience obtained in applications

of hot-wire anemometry in hypersonic flow. An appendix to this report, "Developments in Equipment and Probes for Mean-Flow and Fluctuating-Flow Measurements With a Hot Wire" by Leonard M. Weinstein and John R. Nayadley, Sr., describes some innovations developed for rapid mean flow measurements in hypersonic blow-down wind tunnels.

SYMBOLS

A_w overheat parameter

C wire thermal capacity

d wire diameter

E' finite circuit parameter

e voltage fluctuation across hot wire

Δe_m sensitivity to mass flow

Δe_t sensitivity to stagnation temperature

f frequency

h film coefficient of heat transfer

I hot-wire heating current

$K = \frac{\partial \log R_w}{\partial \log T_w}$

k gas thermal conductivity

l wire length

M Mach number

m mass flow, ρu

$\mathcal{M}$ wire time constant

Nu_t Nusselt number, $\frac{hd}{k_t}$

n_x direction cosine of sound wave front

P_w hot-wire power, I^2R_w

p pressure

Re_t Reynolds number, $\frac{\rho u d}{\mu_t}$

R wire resistance

$R_{mT}, R_{uT}, R_{\rho u}, R_{eT}, R_{\sigma\tau}$ correlation coefficients of indicated fluctuating quantities, for example, $R_{mT} = \frac{\overline{m'T'}}{\tilde{m}\tilde{T}}$

r sensitivity ratio, $\frac{\Delta e_m}{\Delta e_t}$

T temperature

t wedge thickness

u velocity

V hot-wire mean voltage

x,y distances from given reference point

$\alpha = \left(1 + \frac{\gamma - 1}{2} M^2\right)^{-1}$

α_{ref} temperature resistivity coefficient

$\beta = (\gamma - 1)M^2\alpha$

γ ratio of specific heats (1.667 for helium)

ϵ finite circuit factor

η	wire recovery factor $\left(T_w/T_t \text{ at } I = 0\right)$
μ	gas viscosity
$\bar{\pi}$	pressure mode amplitude
ρ	gas density
σ	entropy mode amplitude
τ	vorticity mode amplitude
τ_{wr}	temperature loading, $\frac{T_w - T_r}{T_r}$

Subscripts:

1	ahead of normal shock
2	behind normal shock
a	compensation amplifier setting
e	at edge of turbulent wake
l	local value
o	at center of wake
ref	reference
true	actual value
r	value at $I = 0$
s	source
t	total

w	hot wire
∞	free stream

A tilde over a symbol denotes root mean square; a bar denotes time averaged value; and a prime denotes instantaneous value.

HOT-WIRE INSTRUMENTATION

A diagram of the instrumentation used in the hot-wire measurements is shown in figure 1. The heating circuit, square-wave generator, and compensating amplifier are units of a commercially available constant current anemometer with a frequency response up to 500 kHz. An oscilloscope with a storage mode is used primarily for wire time-constant measurements that are obtained by the square-wave method (ref. 13); the storage mode greatly facilitates these measurements. The variable band-pass filters can be used to improve signal to noise ratio, and two root-mean-square voltmeters are used which have two selectable averaging times, 1/10 and 1/20 of a second. The panoramic wave analyzer permits a quick look and monitoring capability which is important for detecting electrical and strain-gage noise problems. An impedance-matching amplifier with gains of 20 dB and 40 dB is used when tape recording of the hot-wire signals is desired; the tape recorder has a 400 Hz to 1.5 MHz frequency response in the direct record mode and a dc to 400 kHz response in the FM record mode. The mean voltage across and the current through the wire are recorded on a digital recording system or by oscillograph recorders.

The power supply in the heating circuit can be resistance programed, that is, the voltage supplied is proportional to the resistance of a resistor in the power-supply circuit. Different resistors are placed on a solenoid-operated 10-position switch; each position connects a resistor to the voltage supply, and the preselected resistances give different voltages to the heating circuit and, hence, different wire currents. The solenoid which steps the switch can be manually or automatically operated. In the very short running time of about 5 sec in the Langley Mach 20 high Reynolds number helium tunnel, HRNHT (see ref. 14 for a description of this facility), the solenoid is operated by a sequence programer which controls the occurrence of events in the tunnel operation. Figure 2 shows a typical oscillograph record obtained in the HRNHT. About 1.5 sec after start up, when steady-flow conditions are established, the sequence programer begins stepping the resistance switch. The switch stays at each position for about 0.4 to 0.5 sec to obtain good averaging for the root-mean-square voltmeters. (To achieve rapid response of the wire bridge circuit at each position, some changes in the anemometer circuitry were necessary.) At shutdown, the programing resistor is automatically

shorted to give zero voltage from the power supply when the tunnel stagnation pressure drops below 3 percent of the running stagnation pressure; this protects the wire from burnout at shutdown.

PROBE FABRICATION AND CHECKOUT

The hot-wire probes consist of two steel needles (with insulating Teflon sleeves) that were crimped into the flattened tip of a 0.32-cm-diameter piece of stainless-steel tubing (see fig. 3). The needles are about 0.25 cm apart and protrude about 0.5 cm beyond the flattened tube tip. For tests in helium wind tunnels, tungsten wire has been used for the hot wires with wire diameters ranging from 2.54 to 5.08 μm. The ends of the hot wire are first copper plated and then tinned and soft soldered to the needle supports. The length of the unplated wire can be varied in the plating process, and wires with aspect ratios varying from about 150 to 300 have been used. Some detail of the wire mounting can be seen in the photomicrograph in figure 3. The copper plating has a dual purpose: first, to allow the tungsten wire to be soft soldered to the needles and, second, to keep the smaller diameter sensing portion of the wire away from the shock waves of the support needles. Two sets of electrical leads are attached to each needle; one set supplies current to the hot wire, and the other set is used to measure the voltage across the wire.

The wires are mounted with about a quarter circle slack to avoid strain-gage oscillations (see ref. 2) believed to be caused by support-needle vibrations (the exact source is unclear). These strain-gage oscillations are the most troublesome problem experienced in probe construction, and each probe is checked before calibration to assure that it has no strain-gage oscillations when placed in turbulent flow. For this acceptance checking and for general calibrations, a 7.62-cm-exit-diameter conical nozzle that uses helium as a test medium is invaluable (some detail on this nozzle will be given subsequently). At high stagnation pressures, the turbulence in the free stream of this nozzle is sufficient to excite strain-gage oscillations, if they are present. Experience has shown that if strain-gage oscillations are not observed in the small nozzle, they are not observed in the larger test facilities. The hot wires are checked for this effect by recording the spectrum of the hot-wire anemometer voltage from the compensating amplifier with current through the wire. Examples of spectra for a wire with severe strain-gage oscillations and for a wire that is acceptable are shown in figure 4. No visual differences have been observed in the microscope between probes with or without strain-gage oscillations, and the construction of acceptable probes is a trial-and-error process.

Care must also be taken to assure that the support needles are not magnetic. The currents induced by the wire movement in the magnetic field are easily observed as

resonant spikes in the wire-signal spectra, with or without mean current flowing through the wire. Probes showing this effect are degaussed.

CALIBRATIONS

In order to obtain quantitative turbulence measurements, several calibrations of each hot wire are required. The standard calibrations for hot wires (wire temperature versus wire resistance, and heat loss and recovery factor versus flow conditions) must be performed along with an additional calibration for the wire heat capacity; the latter is needed because of the short test times available in the helium test facilities. The procedures for these calibrations will now be discussed.

First, probes which display spectra free of strain-gage oscillations are subjected for several minutes to the maximum stagnation pressure in the 7.62-cm nozzle and an extreme heating current. This procedure is done to prestress the wire to minimize cold resistance changes due to loading. The wires are then calibrated for electrical resistance as a function of temperature in an oven that is pressurized with helium. Pressurized helium is used because air will oxidize the tungsten at the highest temperatures of the oven. The high conductivity of helium also has the beneficial effect of producing a much more uniform temperature in the oven than would occur with air. A typical oven calibration for a tungsten wire is shown in figure 5. Over the temperature range experienced in the helium-tunnel applications, a linear variation of resistance with temperature is quite satisfactory for tungsten wires (less than 1 percent error), or $\gamma_{ref} = 0$ in the equation for the wire electrical resistance (see ref. 2)

$$R_w = R_{ref}\left\{1 + \alpha_{ref}\left(T_w - T_{ref}\right) + \gamma_{ref}\left[\alpha_{ref}\left(T_w - T_{ref}\right)\right]^2\right\} \tag{1}$$

After oven calibration, the wires are calibrated in the flow of the 7.62-cm nozzle for heating rate and recovery-factor variation with flow conditions. The 7.62-cm nozzle can be operated over a range of test conditions which overlap the free-stream conditions of the various Langley hypersonic helium tunnels. A sketch of this nozzle, along with the free-stream conditions $\left(M_\infty \text{ and } Re_t = \frac{\rho_\infty u_\infty d}{\mu_t} \text{ versus stagnation pressure, where } d \text{ is } 2.54\ \mu m\right)$ at the hot-wire calibration station, is shown in figure 6; the free-stream conditions are given at $T_{t,\infty} = 305$ K, a typical operating stagnation temperature which has a slight seasonal variation.

For hypersonic flow the Nusselt number based on stagnation temperature, $Nu_t = \frac{hd}{k_t}$, and the recovery factor, $\eta = \frac{T_r}{T_t}$, are independent of Mach number and depend only upon

the Reynolds number based on stagnation viscosity, $Re_t = \frac{\rho u d}{\mu_t}$, and T_w/T_t. The dependence of Nu_t on T_w/T_t is linear at low overheats (i.e., R_w/R_r less than about 1.25) so that the effect of Re_t on Nu_t can be calibrated by observing the heating rates at low heating currents. The nonlinear effect of T_w/T_t on Nu_t at high overheat is not obtained in the calibration but, following reference 2, is acquired as part of the data that are obtained in actual turbulence measurement with the wire, as will be shown subsequently.

The Nusselt number Nu_t is obtained by equating the ohmic heating to the heat loss by the wire; that is,

$$Nu_t = \frac{hd}{k_t} = \frac{\alpha_{ref} R_{ref} I^2 R_w}{\pi l k_t \left(R_w - R_r\right)} \tag{2}$$

At low overheats and since the power $P_w = I^2 R_w$,

$$Nu_t = \frac{\alpha_{ref} R_{ref}}{\pi l k_t}\left(\frac{dP_w}{dR_w}\right) = Nu_t\left(Re_t\right) \tag{3}$$

For several stagnation pressures, or several Re_t, the power to the hot wire is obtained versus wire resistance, and a linear least-squares-error curve fit to the data is used to find Nu_t. A typical power calibration is shown in figure 7 for a tungsten wire 3.55 μm in diameter and an l/d of about 300. The recovery factor is obtained by observing the resistance for which $P_w = 0$; then using equation (1) to find T_r,

$$\eta = \frac{T_r}{T_t} = \eta\left(Re_t\right) \tag{4}$$

These calibrations (eqs. (3) and (4)) can be used to calculate the hot-wire sensitivity to mass-flow and total-temperature fluctuations. They may also be used to make measurements of the mean flow $\overline{m}$ and $\overline{T}_t$ in unknown flows; measured values of dP_w/dR_w and R_r can be used in an iteration scheme to determine Re_t and T_t and thence $\overline{m}$. In reference 12 such an iteration scheme was used in a Mach 5 free shear layer. Therein, an attempt was made to determine the mean velocity, temperature, and pressure profiles by combining hot-wire measured $\overline{m}$ and $\overline{T}_t$ with measured pitot pressures. In hypersonic flow, this combination of measured variables is rather insensitive to Mach number and is unsatisfactory for mean velocity, temperature, and pressure measurements (see ref. 12 for details). Other mean-flow applications of the hot wire are discussed in the appendix.

Because of the short running times available in the Langley hypersonic helium tunnels, measurements of the hot-wire time constant at each wire operating point is not practical, and an additional calibration (beyond those used in previous lower-speed studies) is performed. Using the standard square-wave technique for determining time constants, the hot-wire time constant is measured at several stagnation pressures in the 7.62-cm nozzle and the theoretical expression developed by Morkovin in reference 2 is used to predict the wire thermal heat capacity C

$$C = \frac{\alpha_{ref} R_{ref} \mathcal{M} I^2 \left(1 + 2\epsilon A_w\right)}{A_w \left[1 - 2\gamma_{ref}\left(R_w - R_r\right)\right]} \tag{5}$$

where Morkovin's overheat parameter is $A_w = \frac{1}{2} \frac{\partial \log R_w}{\partial \log I}$, $\mathcal{M}$ is the time constant, and ϵ is the finite circuit factor. In the calibration, $\mathcal{M}$ is measured only at the highest current since measurements inserted into equation (5) give a constant C versus A_w (to within ±5 percent); see table I for results from a typical wire. Of course, a constant value for C should be obtained. At the low overheats of the calibration, $A_w = \frac{R_w - R_r}{R_r}$ and $\epsilon << 1$; therefore, C is given by (neglecting γ_{ref})

$$C = \alpha_{ref} R_{ref} \mathcal{M} \frac{R_r}{R_w} \left(\frac{dP_w}{dR_w}\right) \tag{6}$$

This equation is used for the C calibration.

A summary of a typical wire calibration is shown in figure 8 which includes data from the small nozzle and from the Langley 22-inch hypersonic helium tunnel (see ref. 15 for a description of this facility). Time-constant measurements were made only at low stagnation pressures in the large facility. The agreement of the calibration data in the two facilities is quite good. The cross-hatched area in the Nu_t calibration is a correlation presented in reference 16 where corrections were applied to account for conduction losses to the support needles. The end loss correction factor is seen to be about 2.0 (measured values of Nu_t divided by the value of Nu_t for an infinite wire) and agrees reasonably well with the theoretical corrections published in reference 17.

The calibrated heat capacity of the wire is nearly constant, as it should be. The average value, $C_{av} = 0.0423 \times 10^{-6}$ J/K, may be compared with a value that was computed using the nominal wire diameter (3.81 μm) and length (1000 μm) and room-temperature material properties. That is,

$$C = \rho_w C_w \frac{\pi}{4} d^2 \ell$$

The computed value is $C = 0.0297 \times 10^{-6}$ J/K, which gives a ratio of measured C to computed C of 1.41. About a 10-percent error (which is reasonable to expect) in both the nominal length and diameter of the wire could account for this discrepancy. Obviously, the cumulative effect of errors in d and l (especially for slack wires) are sufficient cause to reject the use of a computed (from nominal values of d and l) heat capacity for time-constant determinations.

The heat-capacity calibration in figure 8 gives an indication of the accuracy to which the time constant can be determined with the square-wave technique. Even though the actual time constants in the nozzle calibration varied from 350 μsec to 660 μsec over the Re_t range, the maximum scatter in the value of the heat capacity was only ±5 percent as determined in the small nozzle.

DATA REDUCTION

The nearly constant value obtained in the calibration of the wire thermal capacity gives credence to the use of equation (5) to predict the wire time constant once the heat capacity is known. Thus, in the helium tunnels with the short running time (about 50 sec in the 22-inch hypersonic helium tunnel and about 5 sec in the HRNHT), the predicted wire time constant (assuming local mean-flow conditions are known approximately) at an intermediate heating current is set into the hot-wire compensating amplifier at all currents for a single test. The root-mean-square data from the anemometer are then corrected using the formula (see ref. 18)

$$\frac{\tilde{e}_{true}}{\tilde{e}_a} = \frac{\mathcal{M}_{true}}{\mathcal{M}_a} \tag{7}$$

where $\tilde{e}_{true}$ is the rms voltage at the correct time constant $\mathcal{M}_{true}$ and $\tilde{e}_a$ is the rms voltage measured in the test with the intermediate heating current time constant $\mathcal{M}_a$ set in the compensating amplifier. This leads to some signal distortion at low frequencies, on the order of five times the wire roll-off frequency, provided $\mathcal{M}_{true}/\mathcal{M}_a$ is less than about 1.4. Typical wire roll-off frequencies range from 100 Hz to 500 Hz. Applications to date have indicated that the effect of this distortion has been negligible. Thus, thermal inertia effects on the voltage output of the wire were accounted for by: (1) predicting the time constant from the measured heating current I, overheat parameter A_w, and the calibrated thermal capacity C, and (2) correcting the signal according to equation (7).

The output of the compensated hot-wire anemometer as a function of time is, from reference 2,

$$\frac{e'}{V} = \Delta e_t \frac{T_t'}{\bar{T}_t} - \Delta e_m \frac{m'}{\bar{m}} \tag{8}$$

where e', T_t', and m' are the instantaneous fluctuations in wire voltage, total temperature, and mass flow, respectively, and V, $\bar{T}_t$, and $\bar{m}$ are the time averaged values. The wire sensitivities are given by Morkovin in reference 2 as,

$$\Delta e_m = E'\left(A_w \frac{\partial \log Nu_t}{\partial \log Re_t} - \frac{A_w}{\tau_{wr}} \frac{\partial \log \eta}{\partial \log Re_t}\right) \tag{9}$$

and

$$\Delta e_t = E'\left[K + A_w\left(K - 1.647 + 0.647 \frac{\partial \log Nu_t}{\partial \log Re_t} - \frac{0.647}{\tau_{wr}} \frac{\partial \log \eta}{\partial \log Re_t}\right)\right] \tag{10}$$

where the high Mach number independence of Nu_t and η and the helium gas constants have been inserted. The quantity E' is the finite circuit parameter, $\tau_{wr} = \frac{T_w - T_r}{T_r}$ and $K = \frac{\partial \log R_w}{\partial \log T_w}$. The logarithmic derivatives of Nu_t and η are determined from the flow calibrations. Since a good approximation is $Nu_t \propto Re_t^n$, then $\frac{\partial \log Nu_t}{\partial \log Re_t} = n$. Likewise $\frac{\partial \log \eta}{\partial \log Re_t}$ is nearly constant for the Re_t range usually encountered. The value of K is found from the temperature calibration of the wire.

As shown by Morkovin in reference 2, the overheat parameter A_w accounts for nonlinear effects in the variation of Nu_t with T_w/T_t and can be found either graphically or by curve fitting $\log R_w$ in $\log I_w$ for the currents at which the wire is operated. The finite circuit parameter is given by $E' = \frac{1 - \epsilon}{1 + 2A_w\epsilon}$ where $\epsilon = \frac{\partial \log I_w}{\partial \log R_w}$. (Although the system is termed a constant current anemometer, the resistance fluctuations of the wire add to the ballast resistance used to establish the current.)

Modal analysis of the root-mean-square mass-flow and total-temperature fluctuations can be made as suggested by Kovásznay in reference 1 by observing a virtual total total-temperature fluctuation $\frac{\tilde{e}}{V \Delta e_t}$ at several sensitivity ratios $\Delta e_m/\Delta e_t$ (or, in other words, several currents). From equation (8),

$$\left(\frac{\tilde{e}}{V\,\Delta e_t}\right)^2 = \left(\frac{\tilde{T}_t}{\bar{T}_t}\right)^2 - 2r\,\frac{\tilde{T}_t}{\bar{T}_t}\,\frac{\tilde{m}}{\bar{m}}\,R_{mT} + r^2\left(\frac{\tilde{m}}{\bar{m}}\right)^2 \tag{11}$$

where the correlation of mass-flow and total-temperature fluctuations is given as $R_{mT} = \dfrac{\overline{m'T_t'}}{\tilde{m}\tilde{T}_t}$. In each test, the hot wire is operated at about six values of current; this procedure yields redundant information for determining the three unknowns $\tilde{T}_t/\bar{T}_t$, $\tilde{m}/\bar{m}$, and R_{mT} from equation (11) evaluated at each sensitivity ratio (or current).

INTERPRETATION OF FLUCTUATIONS

Interpretation procedures for hot-wire turbulence data have been discussed extensively in the literature (refs. 1, 2, 4, 5, and 19); but a brief review of the procedures will now be made in order to aid in the subsequent discussions of measurements made in the Langley helium tunnels. Since the hot-wire voltage fluctuations are the result of two driving forces, that is, the mass-flow and total-temperature fluctuations, the resolution of the instantaneous signal into the separate contributions of these fluctuations is not possible. But as discussed in the preceding section, one can observe the root mean square of the hot-wire voltage fluctuations at several sensitivity ratios and extract $\tilde{m}/\bar{m}$, $\tilde{T}_t/\bar{T}_t$, and R_{mT} from the data. Unfortunately, these variables cannot be directly interpreted and are not useful to the theoretician in the formulation of flow models or to the designer for calculations dependent upon properties of the flow turbulence. The interpretation of the mass-flow and total-temperature fluctuations in terms of density, pressure, temperature, and velocity fluctuations is the desired result, but in all but a limited number of circumstances this is not possible.

The mass-flow and total-temperature fluctuations are related to the density, temperature, and velocity fluctuations as follows:

$$\frac{T_t'}{\bar{T}_t} = \alpha\,\frac{T'}{\bar{T}} + \beta\,\frac{u'}{\bar{u}} \tag{12a}$$

and

$$\frac{m'}{\bar{m}} = \frac{\rho'}{\bar{\rho}} + \frac{u'}{\bar{u}} \tag{12b}$$

where $\alpha = \left(1 + \dfrac{\gamma - 1}{2}M^2\right)^{-1}$ and $\beta = (\gamma - 1)M^2\alpha$. Hence,

$$\left(\frac{\tilde{T}_t}{\bar{T}_t}\right)^2 = \alpha^2\left(\frac{\tilde{T}}{\bar{T}}\right)^2 + \beta^2\left(\frac{\tilde{u}}{\bar{u}}\right)^2 + 2\alpha\beta\frac{\tilde{T}}{\bar{T}}\frac{\tilde{u}}{\bar{u}}R_{uT} \tag{13a}$$

$$\left(\frac{\tilde{m}}{\bar{m}}\right)^2 = \left(\frac{\tilde{\rho}}{\bar{\rho}}\right)^2 + \left(\frac{\tilde{u}}{\bar{u}}\right)^2 + 2\frac{\tilde{\rho}}{\bar{\rho}}\frac{\tilde{u}}{\bar{u}}R_{\rho u} \tag{13b}$$

$$R_{mT} = \left(\frac{\tilde{m}}{\bar{m}}\frac{\tilde{T}_t}{\bar{T}_t}\right)^{-1}\left\{\alpha\left(\frac{\tilde{\rho}}{\bar{\rho}}\frac{\tilde{T}}{\bar{T}}R_{\rho T} + \frac{\tilde{u}}{\bar{u}}\frac{\tilde{T}}{\bar{T}}R_{uT}\right) + \beta\left[\frac{\tilde{\rho}}{\bar{\rho}}\frac{\tilde{u}}{\bar{u}}R_{\rho u} + \left(\frac{\tilde{u}}{\bar{u}}\right)^2\right]\right\} \tag{13c}$$

Clearly, the density, temperature, and velocity fluctuations cannot be obtained from the measured quantities $\tilde{m}/\bar{m}$, $\tilde{T}_t/\bar{T}_t$, and R_{mT} without some assumption or additional information dealing with the coupling of the density, temperature, and velocity fluctuations. In reference 20 Kovásznay has introduced the concept of fundamental mode variables for compressible turbulent flow and defines entropy, vorticity, and sound modes (σ', τ', and π', respectively), such that

$$\frac{T'}{\bar{T}} = \sigma' + (\gamma - 1)\pi' \tag{14a}$$

$$\frac{u'}{\bar{u}} = \tau' + \left(\frac{n_x}{M}\right)\pi' \tag{14b}$$

$$\frac{p'}{\bar{p}} = \gamma\pi' \tag{14c}$$

It is assumed that the sound mode is a plane wave where n_x is the direction cosine of the sound wave front. In a uniform supersonic flow these three modes of disturbance can independently exist; in shear flows a coupling of the modes will occur. Each mode alone gives a unique hot-wire mode diagram (see ref. 19). These three mode diagrams are given by (from eqs. (11) to (14))

Entropy

$$\frac{\tilde{e}}{V\,\Delta e_t} = (r + \alpha)\tilde{\sigma}$$

Vorticity

$$\frac{\tilde{e}}{V\,\Delta e_t} = +(\beta - r)\tau \qquad \text{(for } \beta - r > 0\text{)}$$

$$\frac{\tilde{e}}{V\,\Delta e_t} = -(\beta - r)\tau \qquad \text{(for } \beta - r < 0\text{)}$$

Sound

$$\frac{\tilde{e}}{V\,\Delta e_t} = \alpha(\gamma - 1)\left(M^2\,\frac{\tilde{u}}{\bar{u}} - \tilde{\pi}\right) + \left(\tilde{\pi} - \frac{\tilde{u}}{\bar{u}}\right)r$$

For the sound mode, $\tilde{u}/\bar{u}$ is the root mean square of the mean-flow direction component of the velocity fluctuations normal to the sound-wave front

$$\left(\frac{\tilde{u}}{\bar{u}}\right)^2 = \frac{\tilde{\pi}^2}{M^2}\,n_x^{\,2} \tag{15}$$

Although each of these diagrams consists of straight lines, the unique features of the diagrams allow identification of individual modes in flows. For example, the vorticity diagram initially has a negative slope (with respect to the sensitivity r) followed by a straight-line branch with positive slope beyond $r = \beta$, and all entropy diagrams are single straight lines which pass through $\frac{\tilde{e}}{V\,\Delta e_t} = 0$ at $r = -\alpha$, with positive slope.

For two co-existing modes (assuming the wave-front orientation is known in the case of one mode being the sound mode), the measured quantities can be used to calculate the mode variables and their correlation (for example, $\tilde{\sigma}$, $\tilde{\tau}$, and $R_{\sigma\tau}$) and hence the fluctuations in flow quantities (for example, $\tilde{\rho}$, $\tilde{u}$, and $\tilde{T}$, and their correlations). When more than two modes exist, then the resolution of the measured fluctuations into the levels of fluctuation of the flow variables is not possible without some assumptions concerning the coupling of modes. Laderman and Demetriades (ref. 5) have, for example, employed the following assumptions in a hypersonic turbulent boundary layer (where all three modes should be present): (1) the sound mode is uncorrelated with vorticity and entropy modes ($R_{\pi\tau}$ and $R_{\pi\sigma} = 0$) and (2) $R_{\sigma\tau} = -1$. Since the mechanics of sound propagation and vorticity and entropy diffusion are physically different, the first assumption should be valid in uniform flows without shear. If the turbulence is visualized as moving eddies, then the slower moving eddies should have greater entropy, and vice versa, so that σ' and τ' will be anticorrelated. However, as Lighthill's acoustic analogy shows (see ref. 21), the sound radiated away from a turbulent shear flow comes about because of the turbulent fluctuations in the shear layer, and hence surely in the shear layer π, σ, and τ must have some correlation. Also Laderman and Demetriades' scheme (ref. 5) incorporates the assumption of plane sound waves with $n_x = -\frac{1}{M}$; within the sound producing shear layer, this assumption of locally plane waves must be violated. Thus, this

scheme seems to have physically doubtful applicability. It appears that, in order for the hot wire to be truly useful in hypersonic turbulent shear flows where mixed modes are believed to occur, an additional measurement must be made that will yield information on a flow variable other than m' or T_t'; this appears to be an impasse to extended applications of hypersonic hot-wire anemometry. In all applications to be discussed subsequently, the turbulence in the flows was judged to be predominantly caused by fluctuations from one mode.

APPLICATIONS

Free-Stream Disturbance Measurements

Most of the hot-wire applications made in the Langley helium tunnels have been in programs concerned with the effects of the facility disturbance environment on model boundary-layer transition. The disturbance environment has been measured in two Langley hypersonic helium tunnels (refs. 6 and 9), the 22-inch hypersonic helium tunnel and the Mach 20 high Reynolds number helium tunnel (HRNHT); these facilities are described in references 15 and 14, respectively. Disturbance measurements have been made using the mode-diagram approach, and mode diagrams obtained in the free stream of the HRNHT are shown in figure 9. The measurements were made near the tunnel center line, since previous studies have shown uniform disturbance intensity outside the nozzle-wall boundary layers in hypersonic tunnels. These measurements were obtained using a tungsten wire, 4.70×10^{-4} cm in diameter, with an aspect ratio of about 200. All the data were obtained (stepping through the voltage programer) in the last 3 sec of the 5-sec running time. Steady flow was established at the prescribed stagnation pressure within the first 2 sec.

A number of reruns shown in figure 9 gives an indication of the repeatability that can be obtained with a single wire. The worst deviation in the data from the mean is less than 10 percent, and in four of the seven cases with reruns the two data sets give nearly identical results.

Within the data scatter, all the mode diagrams are linear. As shown in reference 19 and as discussed in the section entitled "Interpretation of Fluctuations," this fact, along with the examination of the diagram intercepts at $r = 0$, allows interpretation of the disturbances as sound waves having a preferred orientation and radiated from a moving source, the turbulent nozzle-wall boundary layer. From equation (11), since the mode diagrams are linear, $R_{mT} = -1$ and

$$\frac{\tilde{e}}{V\,\Delta e_t} = \frac{\tilde{T}_t}{\bar{T}_t} + r\,\frac{\tilde{m}}{\bar{m}}$$

that is, the slopes of the mode diagrams give the root mean square of the mass-flow fluctuations and the intercepts at $r = 0$ give the root mean square of the total-temperature fluctuations. These quantities are shown in figure 10. The mass-flow fluctuations are quite intense compared with those existing in lower speed tunnels, becoming as much as about 3 percent at the lower stagnation pressures. The total-temperature fluctuations are two orders of magnitude smaller than the mass-flow fluctuations and are about constant over the operating pressure range.

In reference 19 Laufer shows how $\tilde{m}/\bar{m}$ and $\tilde{T}_t/\bar{T}_t$ may be used to calculate the root mean square of the pressure fluctuations and the source velocity of the radiated pressure fields. For high Mach numbers and small total-temperature fluctuations, a good approximation is

$$\frac{\tilde{p}}{\bar{p}} = \frac{\gamma \tilde{m}}{\bar{m}} \tag{16}$$

and this relation has been used to insert the $\tilde{p}/\bar{p}$ scale shown in figure 10. The source-velocity scale in the graph of total-temperature fluctuations shows a nearly constant source velocity with $\frac{u_s}{u_\infty} \approx 0.66$. This value is only slightly greater than the value of $\frac{u_s}{u_\infty} \approx 0.56$ found by Laufer in reference 22 at $M_\infty = 5$; Laufer also observed a trend of increasing source velocity with Mach number.

Source-velocity measurements from hot-wire mode diagrams in hypersonic flow must be considered with caution in view of a considerable margin of uncertainty resulting because of an inherent limitation of the hot wire in hypersonic flow. In hypersonic flow, for plane sound waves $\tilde{T}_t/\bar{T}_t$, $\tilde{m}/\bar{m}$, and u_s/u_∞ are related as follows (see ref. 6):

$$\frac{\tilde{T}_t}{\bar{T}_t} \approx \frac{2 \frac{u_s}{u_\infty} \frac{\tilde{m}}{\bar{m}}}{M_\infty^2 \left(1 - \frac{u_s}{u_\infty}\right)}$$

Figure 11 shows the relation between $\tilde{T}_t/\bar{T}_t$, u_s/u_∞, and $\tilde{m}/\bar{m}$ and M_∞. If a minimum resolvable $\tilde{T}_t/\bar{T}_t$ error (which would be about 0.02 for the present tests) is selected, the corresponding source-velocity error is quite large at small source velocities and small at large source velocities. Thus the source-velocity resolution is quite poor except for sources moving near stream velocity. This may be explained physically as follows. The total temperature fluctuations indicated by the hot wire in a sound disturbance come about because of the velocity fluctuations present. These fluctuations are

normal to the wave fronts, the inclination of which depends on the source velocity since the sound radiates intensely at the relative Mach angle. The hot wire is sensitive only to velocity fluctuations in the mean-flow direction; therefore, for slow moving sources where the wave fronts are nearly parallel to the mean flow (in hypersonic flow), the hot wire becomes insensitive to the velocity fluctuation and, hence, the wave-front orientation (or source velocity) cannot be resolved. In fact, it becomes very difficult in hypersonic flow to distinguish between disturbances that are entropy fluctuations and sound from a slow moving source because the velocity fluctuations in the latter are the only distinguishing feature and the hot wire senses only a small component of the velocity fluctuation because of the shallow wave fronts. For entropy disturbances, the hot-wire response is given by (see section entitled "Interpretation of Fluctuations")

$$\frac{\tilde{e}}{V\,\Delta e_t} = (r + \alpha)\tilde{\sigma}$$

where $\tilde{\sigma}$ is the root mean square of the entropy fluctuations. The entropy mode diagram is therefore linear with $\frac{\tilde{e}}{V\,\Delta e_t} = 0$ at $r = -\alpha$. The quantity α rapidly approaches zero as Mach number increases; hence, the mode diagrams for sound waves produced by slow moving sources and entropy disturbances become nearly identical for hypersonic flow.

Pressure-fluctuation levels obtained in the HRNHT and the 22-inch hypersonic helium tunnel were calculated using equation (16) and are compared in figure 12. In reference 6 it is shown that the rapid increase in $\tilde{p}/\bar{p}_\infty$ at low stagnation pressures in the 22-inch tunnel is caused by transition of the nozzle-wall boundary layer from laminar to turbulent flow; above $p_{t,1} \approx 3$ MN/m^3 the nozzle-wall boundary layer is turbulent and radiates sound into the free stream. In the HRNHT, turbulent boundary layers exist on the nozzle wall over the operating pressure range. In both tunnels, with turbulent nozzle-wall boundary layers, the root mean square of the pressure fluctuations (in percent of free-stream static pressure) decreases with increasing stagnation pressure (or unit Reynolds number); this trend is consistent with the results obtained by Laufer in reference 19. The levels of the root mean square of the pressure fluctuations are quite high, up to 6 percent which is as much as 3 times higher than those measured by Laufer at $M_\infty = 5$.

The source-velocity measurements in the 22-inch tunnel indicate the variation of u_s/u_∞ going from 0 to near 1 over the operating pressure range, but the previously discussed uncertainty (see fig. 12) is very large except at the highest stagnation pressure. It is not understood why the source-velocity values at the high pressures do not agree

with those values measured in the HRNHT since the sidewall boundary layers are both turbulent at these pressures and the free-stream Mach numbers are nearly equal.

The relative magnitudes of $\tilde{m}/\bar{m}$ and $\tilde{T}_t/\bar{T}_t$ obtained in these unheated helium tunnels ($\tilde{m}/\bar{m}$ at least two orders of magnitude larger than $\tilde{T}_t/\bar{T}_t$) leads to another problem with the hot wire in these hypersonic flows, namely, poor resolution of R_{mT}. For $\frac{\tilde{m}}{\bar{m}} >> \frac{\tilde{T}_t}{\bar{T}_t}$ and at high overheat (large r), where the signal-to-noise ratio is best,

$$\frac{\tilde{e}}{V\,\Delta e_t} \approx r\,\frac{\tilde{m}}{\bar{m}}$$

or, all mode diagrams have this asymptote, regardless of the disturbance nature. The minimum value of $\frac{\tilde{e}}{V\,\Delta e_t}$ can be found from equation (11) to be at

$$r_{min} = \left(\frac{\tilde{T}_t/\bar{T}_t}{\tilde{m}/\bar{m}}\right) R_{mT}$$

Since $|R_{mT}| \leq 1$, then

$$|r_{min}| = O\left(\frac{\tilde{T}_t/\bar{T}_t}{\tilde{m}/\bar{m}}\right)$$

or if $\tilde{T}_t/\bar{T}_t << \tilde{m}/\bar{m}$, then r (and hence the overheat) is nearly zero where the minimum occurs and, thus, the signal-to-noise ratio is poor. It is near this minimum that the mode-diagram features, which yield information on R_{mT} (or the disturbance nature), are found. Because of the poor signal-to-noise ratio for small sensitivity ratio, resolution of these features is very difficult. This result also illustrates a basic limitation of the constant-temperature anemometer for hypersonic flows in which the total-temperature fluctuations are small compared with the mass-flow fluctuations. At the low overheats needed to resolve R_{mT} the constant-temperature anemometer may have inadequate frequency response. The upper frequency-response limit of the constant-temperature anemometer varies with the wire overheat; this limit varies from the wire roll-off frequency at low overheats to the maximum attainable by the feedback network at high overheats when sufficient power is delivered to the wire (see ref. 23).

On the other hand, however, the small total-temperature fluctuations present can lead to some useful approximations. In this case, if $\frac{\partial \log \eta}{\partial \log Re_t} \approx 0$, which is a good approximation for $Re_t > 1$, and if $\frac{\partial \log Nu_t}{\partial \log Re_t} = n$ which is also a good approximation over a wide Re_t range, then (assuming $\epsilon \approx 0$ and $E' \approx 1$)

$$\Delta e_m \approx nA_w$$

or

$$\frac{\tilde{e}}{V} \approx \left(\frac{\tilde{m}}{\bar{m}}\right) nA_w$$

Since the amplifier output e_a is measured and since $\tilde{e} \approx \tilde{e}_a\left(\mathcal{M}/\mathcal{M}_a\right)$ where $\mathcal{M} \approx \frac{C}{\alpha_r R_r} \frac{A_w}{I^2}$, then it is easily shown that

$$\frac{\tilde{m}}{\bar{m}} \approx \frac{\tilde{e}_a}{V} \frac{C}{\mathcal{M}_a \alpha_r R_r} \frac{1}{nI^2}$$

If relative intensity measurements are desired, then for a given wire

$$\frac{\left(\tilde{m}/\bar{m}\right)_1}{\left(\tilde{m}/\bar{m}\right)_2} \approx \left[\frac{\left(\tilde{e}_a/V\right)_1}{\left(\tilde{e}_a/V\right)_2}\right]\left(\frac{I_2}{I_1}\right)^2 \frac{\mathcal{M}_{a,2}}{\mathcal{M}_{a,1}}$$

or if the amplifier time constant and current are held fixed, then

$$\frac{\left(\tilde{m}/\bar{m}\right)_1}{\left(\tilde{m}/\bar{m}\right)_2} \approx \frac{\left(\tilde{e}_a/V\right)_1}{\left(\tilde{e}_a/V\right)_2}$$

This is a quite useful relation, since it shows that for relative measurements, a calibration of the hot wire is not necessary, even for $R_w = R_w\left(T_w\right)$. If the mean flow is uniform

$$\frac{\tilde{m}_1}{\tilde{m}_2} \approx \frac{\tilde{e}_{a,1}}{\tilde{e}_{a,2}}$$

Hypersonic Wake Flow

Some measurements obtained in the wake produced by a 15° half-angle wedge in a helium tunnel at $M_{\infty} = 15.5$ are shown in figure 13. (This tunnel has a contoured nozzle which expands into a constant-diameter test section, 0.61 m in diameter.) The wedge was 1.905 cm thick at the base and spanned a section of the nozzle 35.6 cm in diameter. The potential core of the nozzle is about 25.4 cm at this section. The wedge was cooled to near the wedge adiabatic wall temperature before the tests so as to have near adiabatic flow.

The results obtained from a survey through the turbulent wake at 68.3 wedge thicknesses downstream of the wedge base is shown in figure 13. Shown are pitot pressure, total temperature (obtained with a shielded iron-constantan thermocouple probe), and hot-wire data profiles. The hot-wire data profiles were taken with a tungsten wire at a fixed current; the mean wire voltage and the root mean square of the compensated wire-voltage fluctuations are shown. The root-mean-square voltage profile displays two regions of intense disturbances to either side of the wake center line and virtually no signal above the instrument noise outside of the turbulent wake.

The wake is judged to be turbulent for two reasons. First, a considerable disturbance level exists on the center line much above the instrument noise level; this is indicative that transition has occurred far upstream in the wake (see ref. 24). Secondly, mode diagrams (which will be discussed subsequently) of the signals at the wake center line and at the peak root-mean-square point indicate that the root mean square of the mass-flow fluctuations are 6.2 and 10.9 percent of the mean mass flow, respectively; surely disturbances this intense cannot be consistent with laminar flow.

At the edge of the turbulent wake the pitot pressure is very near the pitot pressure, $p_{t,2}(\infty)$, which would be observed for expansion of the wedge flow back to stream static pressure in the far wake (assuming that the entropy change is small across the wake recompression shock as it should be). The turbulent-wake edge Mach number should then be about 9.6. Through the hypersonic approximation for the Rayleigh pitot formula, assuming constant static pressure through the turbulent wake (see ref. 25), an approximate Mach number variation through the wake can be determined from the data by

$$\frac{p_{t,2,l}}{p_{t,2,e}} \approx \frac{M_l^2}{M_e^2}$$

The center-line Mach number is about 7. Since the total temperature is nearly constant, dropping only 5 K from wake edge to wake center, the velocity defect in the wake must be nearly "washed" out at this station and the velocity defect can be estimated from the energy equation to be

$$\frac{u_e - u_o}{u_e} \approx 0.015$$

therefore, the turbulent wake shows primarily a density defect of

$$\frac{\rho_e - \rho_o}{\rho_e} \approx 0.45$$

One might then expect that the wake turbulence is predominantly due to density fluctuations. This premise can be examined using the mode-diagram approach.

Two mode diagrams were taken: one at the wake center line, $y = 0$, and one at a position of peak root-mean-square voltage fluctuation, $y = 1.68$ cm, in figure 13. These mode diagrams are shown in figure 14. Both mode diagrams are linear within the accuracy of the measurements; hence, R_{mT} is -1 and the computed $\tilde{m}/\bar{m}$ and $\tilde{T}_t/\bar{T}_t$ are indicated in figure 14. This value of R_{mT} is consistent with the disturbances being either sound or entropy fluctuations (see ref. 2). Sound can be eliminated since no signal above the instrument noise is observed at the wake edge; if sound were present, radiation into the flow about the wake would be expected. For entropy fluctuations, the mode diagrams are given by (see section entitled "Interpretation of Fluctuations")

$$\frac{\tilde{e}}{V\,\Delta e_t} = (r + \alpha)\frac{\tilde{\rho}}{\bar{\rho}}$$

which (as previously noted), in addition to implying a linear mode diagram, dictates that at $r = -\alpha$,

$$\frac{\tilde{e}}{V\,\Delta e_t} = 0$$

From Mach number estimates based on pitot-pressure ratios, the local values of α were computed and are shown in figure 14. Each mode diagram passes through $\frac{\tilde{e}}{V\,\Delta e_t} = 0$ near the corresponding computed value of α. It can then be concluded that the disturbances belong to the entropy-mode type. As Morkovin points out in reference 2, the entropy mode must consist of a moving frozen pattern of entropy, density, and temperature variation preset by the conditions upstream where mixing has occurred.

Another interesting observation is that, as previously noted, no signal above the instrument noise is observed outside of the turbulent wake. Since the wake turbulence should be convected with near local velocity and the velocity defect is very small, eddy

Mach wave radiation of sound from the turbulence will not occur. But still some signal in the flow external to the wake might be expected; the sound radiated from the turbulent nozzle-wall boundary layers should radiate through the free stream and penetrate the inviscid wake. Apparently, this penetration does not occur. This radiation is possibly reflected by the inviscid wake because of the high local static temperatures and, hence, higher local sonic velocities. (For $M_e = 9.6$, the ratio of the local static temperature to the free-stream static temperature would be 2.4.)

CONCLUDING REMARKS

Hot-wire anemometry techniques have been successfully applied to make turbulence measurements in hypersonic helium flows. Although the hot-wire technique has some basic limitations in helium flows with small total-temperature fluctuations, much information can be obtained. The helium tunnel offers a unique facility wherein hypersonic turbulence can be studied without the hot-wire fabrication problems encountered in applications in the high temperature, hypersonic-air wind tunnels.

Langley Research Center,
National Aeronautics and Space Administration,
Hampton, Va., January 28, 1974.

APPENDIX

DEVELOPMENTS IN EQUIPMENT AND PROBES FOR MEAN-FLOW AND FLUCTUATING-FLOW MEASUREMENTS WITH A HOT WIRE

By Leonard M. Weinstein and John R. Nayadley, Sr.
Langley Research Center

Mean-flow measurements using a hot-wire anemometer have been made in model and tunnel wall boundary layers in the Langley hypersonic helium tunnels (refs. 7 and 26). These measurements impose stringent requirements on instrumentation due to the large gradients through the thin boundary layers (approximately 1 cm for ref. 26) and short run time (approximately 3 sec). For example, the density changed by a factor of 100 through the $M_e = 20$ boundary layers (ref. 7). Since the number of runs possible in a day was small (say, four per day in the HRNHT), complete boundary-layer surveys had to be made in one or two runs to keep test time reasonable. In reference 26, two runs were made at each boundary-layer station to obtain mean data. In one the wire was hot, and for the other the wire was used as a resistance thermometer. These allowed determination of m and T_t as was indicated in the body of this paper. Since the heated wire had to be at a reasonably constant temperature through the survey, a constant-temperature anemometer was used to heat the probe. The modifications that were made to a conventional hot-wire apparatus to meet these requirements of short-run times and steep spatial gradients are given in the following section.

Additions to Hot-Wire Instrumentation System

For those studies where even the slight change of stagnation conditions from run to run is unacceptable, or if the available test time is short, a method was developed to obtain both heated and unheated mean wire data profiles in a single run. A sketch of the instrumentation is shown in figure 15(a). As the probe traversed, a two-position switch alternates between constant-temperature and resistance-thermometer modes of operation. The switching unit consists of a solid-state bistable multivibrator which operates a miniature, fast acting relay. It is triggered by the master synchronous clock signal. The wire is typically switched 10 times per sec, and the data are encoded by an analog to digital converter (A/D converter) with a 9 ms average time. The digital data are recorded on a digital tape recorder. Alternate data points are faired to give two profiles in the single run, and values from the fairings at a given height are used to obtain m and T_t.

There are some studies where the fluctuating data at one overheat, as well as mean data, are desired in a survey. For these cases the constant-temperature anemometer does not have adequate frequency response. In addition, when the hot wire is used to

examine fluctuating quantities in unknown flows, it may be difficult to correctly estimate the power needed to obtain a given overheat. For these reasons, the instrumentation shown in figure 15(b) was developed. The constant-current anemometer power supply is resistance programed by a photoconductor which is included in the closed-loop electronic servosystem. Changes in hot-wire resistance controls the power-supply output to maintain a constant-temperature condition. As the frequency response of the control system is limited to about 10 Hz, the system responds only to changes in the mean flow; thus a preselected temperature is automatically maintained through a survey.

The wire current and voltage are measured, as well as the fluctuating output, and the fluctuation level is adjusted for incorrect time-constant effects by equation (7). The time-constant set is that which compensates the output to 500 kHz, and generally the signal is undistorted to below 1 kHz. This bandwidth is adequate for most studies of the helium tunnels.

The temperature-controlled constant-current anemometer can also be used for mean-flow measurements instead of the constant temperature one and thus the observer can use a single system for a wide variety of tests.

Special Hot-Wire Probes

Although the conventional hot wire can be used to obtain the local total temperature, the procedure is difficult and requires an iteration of results from several data points. In reference 26, the procedure was simplified somewhat by using only two data points and fairing a straight line between the two, but an iteration procedure was still required. For the cases where only T_t is needed and where probe size is not so critical, the simple shielded thermocouple probe is often used. There are cases where the wire response and error due to end losses of thermocouple probes limit data accuracy. To overcome this limit, the shielded fine-wire probe of reference 27 was developed. This probe is faster responding and more accurate than shielded thermocouple probes. The end-loss correction still requires an approximate Reynolds number, and the probe is still limited in accuracy for uncorrected use. By using a coil-wire sensing element with a very high ratio of l/d, losses in this probe are minimized and good accuracy with no correction is possible. The coil-wire probe described in reference 28 (both unshielded and shielded) was developed to overcome several limitations of a conventional wire. A small coil of tungsten wire (from a light bulb) was copper plated at the ends, stretched across notched needles, and soft soldered to the needle tips. The needles were held in a Teflon insulator within a small steel tube. A sketch of a typical probe is shown in figure 16(a) and a photomicrograph of one of the coil probes is shown in figure 16(b). The probe shown had a wire diameter of 0.0025 cm, and a coil diameter of 0.013 cm, and a true-wire ratio (l/d) of 400. The spring-like properties of the coil allow a higher length-to-diameter

ratio wire for a given flow. In addition, the coil is more rugged for sudden flow changes. The coil wire seems to be free of strain-gage effects for moderately large ratios l/d, and hence the coil can be mounted straight across the support tips, and thus the support interference is minimized. The coil-wire probe can be used like a conventional wire, and a dual swept-coil probe can be used to measure flow angle. The coil diameter is large compared with a conventional wire, but still smaller than any shrouded probe. The intermediate size results in probe Knudsen numbers more nearly continuum than for a straight wire, and thus lower corrections are necessary than for conventional unshielded wires.

REFERENCES

1. Kovásznay, Leslie S. G.: The Hot-Wire Anemometer in Supersonic Flow. J. Aeronaut. Sci., vol. 17, no. 9, Sept. 1950, pp. 565-572, 584.

2. Morkovin, Mark V.: Fluctuations and Hot-Wire Anemometry in Compressible Flows. AGARDograph 24, Nov. 1956.

3. Laufer, John; and Vrebalovich, Thomas: Stability and Transition of a Supersonic Laminar Boundary Layer on an Insulated Flat Plate. J. Fluid Mech., vol. 9, pt. 2, Oct. 1960, pp. 257-299.

4. Kistler, Alan L.: Fluctuation Measurements in Supersonic Turbulent Boundary Layers. Rept. No. 1052, Ballistic Res. Lab., Aberdeen Proving Ground, Aug. 1958.

5. Laderman, A. J.; and Demetriades, Anthony: Hot-Wire Measurements of Hypersonic Boundary-Layer Turbulence. Phys. Fluids, vol. 16, no. 2, Feb. 1973, pp. 179-181.

6. Wagner, R. D., Jr.; Maddalon, D. V.; and Weinstein, L. M.: Influence of Measured Freestream Disturbances on Hypersonic Boundary-Layer Transition. AIAA J., vol. 8, no. 9, Sept. 1970, pp. 1664-1670.

7. Fischer, M. C.; Maddalon, D. V.; Weinstein, L. M.; and Wagner, R. D., Jr.: Boundary-Layer Pitot and Hot-Wire Surveys at $M_\infty = 20$. AIAA J., vol. 9, no. 5, May 1971, pp. 826-834.

8. Fischer, M. C.; and Wagner, R. D.: Transition and Hot-Wire Measurements in Hypersonic Helium Flow. AIAA J., vol. 10, no. 10, Oct. 1972, pp. 1326-1332.

9. Wagner, R. D.: Hot Wire Measurements of Freestream and Shock Layer Disturbances. AIAA J., vol. 9, no. 12, Dec. 1971, pp. 2468-2470.

10. Stainback, P. C.; and Wagner, R. D.: A Comparison of Disturbance Levels Measured in Hypersonic Tunnels Using a Hot-Wire Anemometer and a Pitot Pressure Probe. AIAA Paper No. 72-1003, Sept. 1972.

11. Weinstein, Leonard M.: Oblique Shock-Sound Interaction at $M_\infty \simeq 20$ in Helium. AIAA J., vol. 10, no. 12, Dec. 1972, pp. 1718-1720.

12. Wagner, R. D.: Mean Flow and Turbulence Measurements in a Mach 5 Free Shear Layer. NASA TN D-7366, 1973.

13. Kovasznay, Laszlo: Calibration and Measurement in Turbulence Research by the Hot-Wire Method. NACA TM 1130, 1947.

14. Watson, Ralph D.; and Bushnell, Dennis M.: Calibration of the Langley Mach 20 High Reynolds Number Helium Tunnel Including Diffuser Measurements. NASA TM X-2353, 1971.

15. Arrington, James P.; Joiner, Roy C., Jr.; and Henderson, Arthur, Jr.: Longitudinal Characteristics of Several Configurations at Hypersonic Mach Numbers in Conical Contoured Nozzles. NASA TN D-2498, 1964.

16. Weltmann, Ruth N.; and Kuhns, Perry W.: Heat Transfer to Cylinders in Crossflow in Hypersonic Rarefied Gas Streams. NASA TN D-267, 1960.

17. Dewey, C. Forbes, Jr.: Hot-Wire Measurements in Low Reynolds Number Hypersonic Flows. Hypersonic Res. Proj. Mem. No. 63 (Contracts DA-04-495-Ord-1960 and DA-04-495-ORD-3231), Guggenheim Aeronaut. Lab., California Inst. Technol., Sept. 15, 1961.

18. Morkovin, Mark V.; and Phinney, Ralph E.: Extended Applications of Hot-Wire Anemometry to High-Speed Turbulent Boundary Layers. AFOSR TN-58-469, DDC No. 158-279, June 1958.

19. Laufer, John: Aerodynamic Noise in Supersonic Wind Tunnels. J. Aerosp. Sci., vol. 28, no. 9, Sept. 1961, pp. 685-692.

20. Kovásznay, Leslie S. G.: Turbulence in Supersonic Flow. J. Aeronaut. Sci., vol. 20, no. 10, Oct. 1953, pp. 657-674, 682.

21. Lighthill, M. J.: Sound Generated Aerodynamically. Proc. Roy. Soc. London, Ser. A, vol. 267, no. 1329, May 8, 1962, pp. 147-182.

22. Laufer, John: Sound Radiation From a Turbulent Boundary Layer. Tech. Rep. No. 32-119 (Contract No. NASw-6), Jet Propulsion Lab., California Inst. Technol., Nov. 1, 1961.

23. Hinze, J. O.: Turbulence. McGraw-Hill Book Co., Inc., 1959.

24. Demetriades, Anthony: Hot-Wire Measurements in the Hypersonic Wakes of Slender Bodies. AIAA J., vol. 2, no. 2, Feb. 1964, pp. 245-250.

25. Batt, Richard George: Experimental Investigation of Wakes Behind Two-Dimensional Slender Bodies at Mach Number Six. Ph. D. Thesis, California Inst. Technol., 1967.

26. Fischer, Michael C.; and Weinstein, Leonard M.: Three-Dimensional Hypersonic Transitional/Turbulent Mean Flow Profiles on a Slender Cone at Angle of Attack. AIAA Paper No. 73-635, July 1973.

27. Weinstein, Leonard M.: A Shielded Fine-Wire Probe for Rapid Measurements of Total Temperature in High-Speed Flows. J. Spacecraft & Rockets, vol. 8, no. 4, Apr. 1971, pp. 425-428.

28. Weinstein, Leonard M.: A Hot-Wire Coil Probe for High-Speed Flows. AIAA J., vol. 11, no. 12, Dec. 1973, pp. 1772-1773.

TABLE I.- HEAT-CAPACITY MEASUREMENTS

AT DIFFERENT OVERHEATS

A_w	C/C_{av}
0.052	0.957
.096	1.005
.153	1.042
.245	1.035
.312	1.021
.395	.954
.465	.983

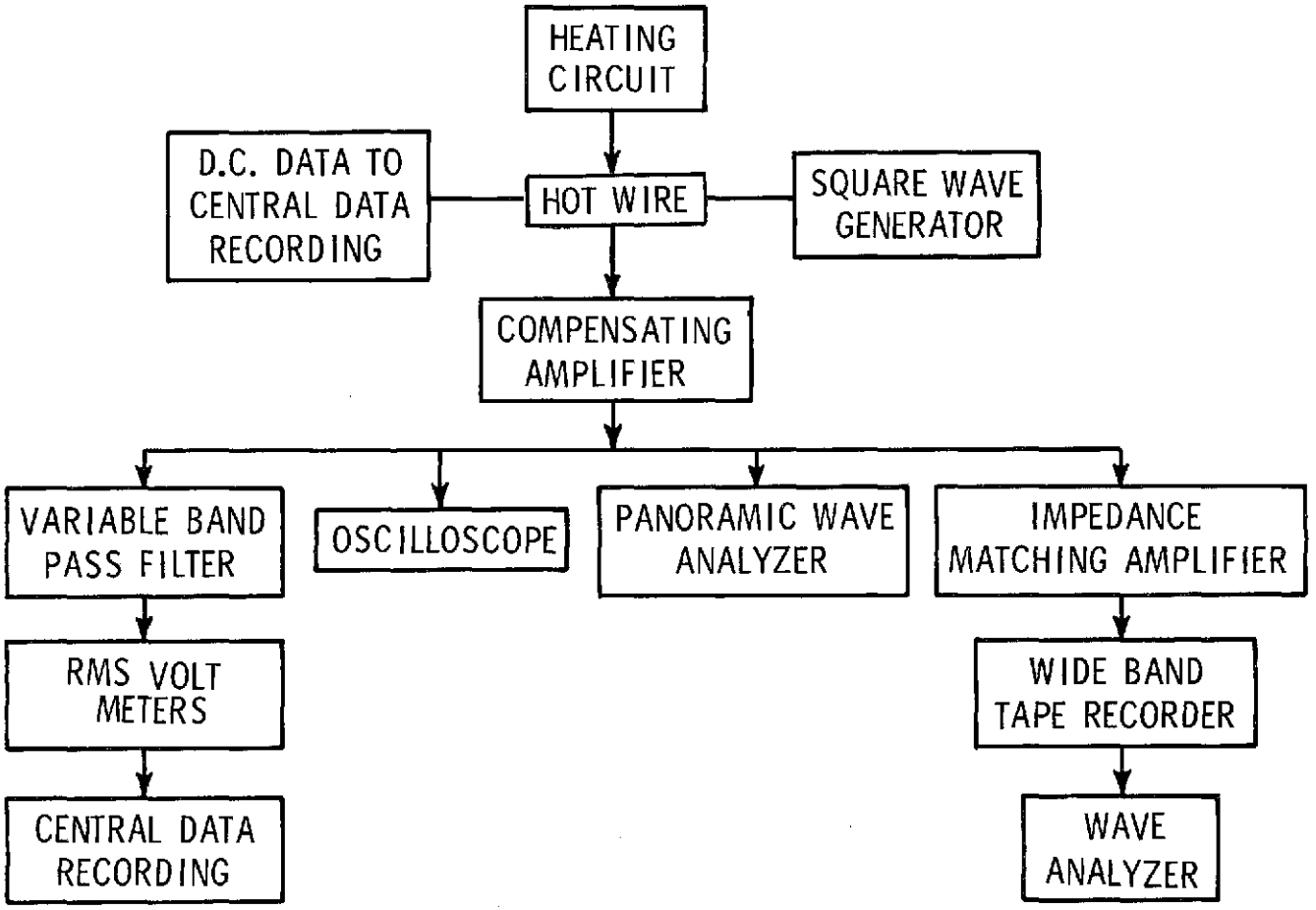

Figure 1.- Instrumentation diagram.

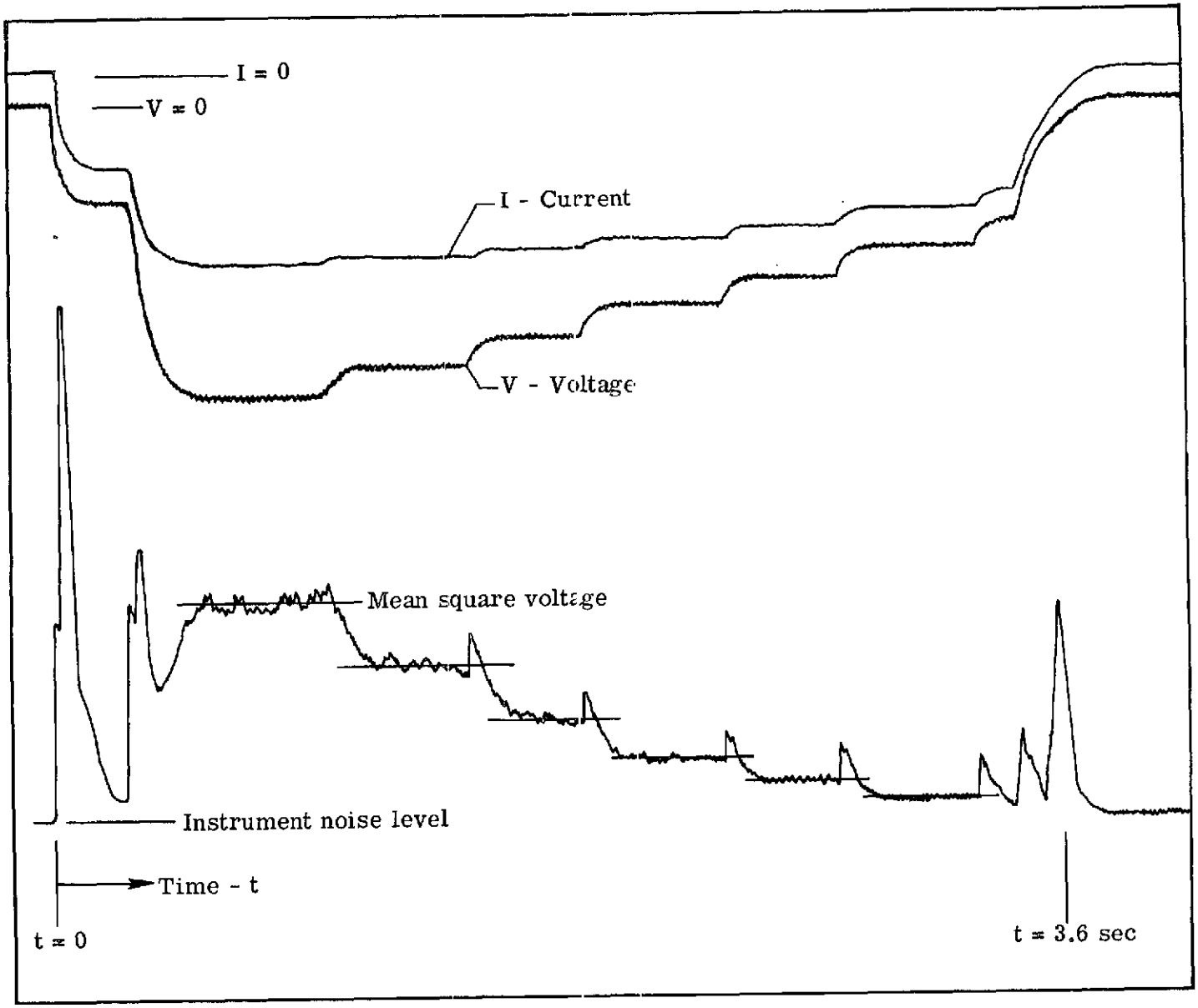

Figure 2.- Oscillograph record of hot-wire signals.

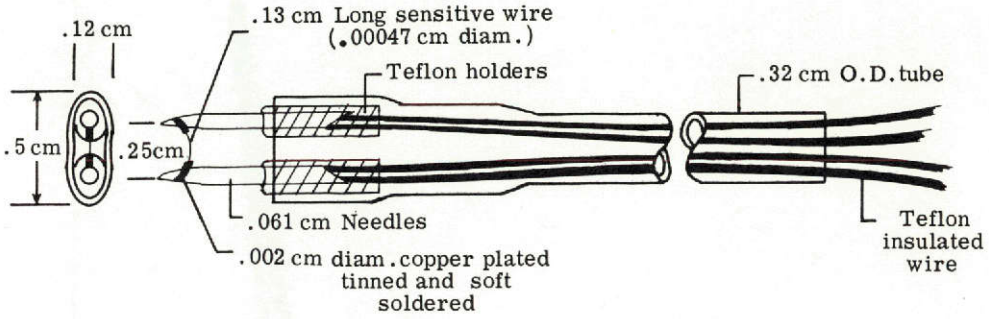

(a) Sketch of hot-wire probe.

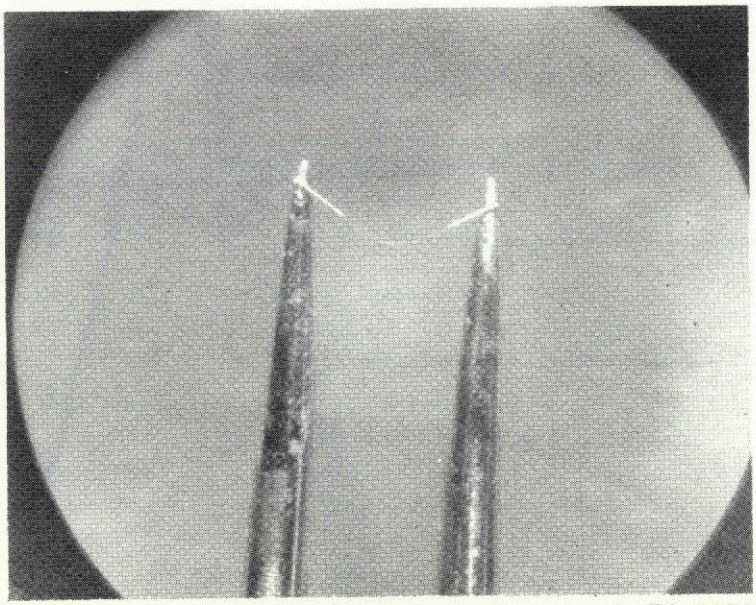

L-74-1072

(b) Photomicrograph of mounted wire.

Figure 3.- Hot-wire probe construction.

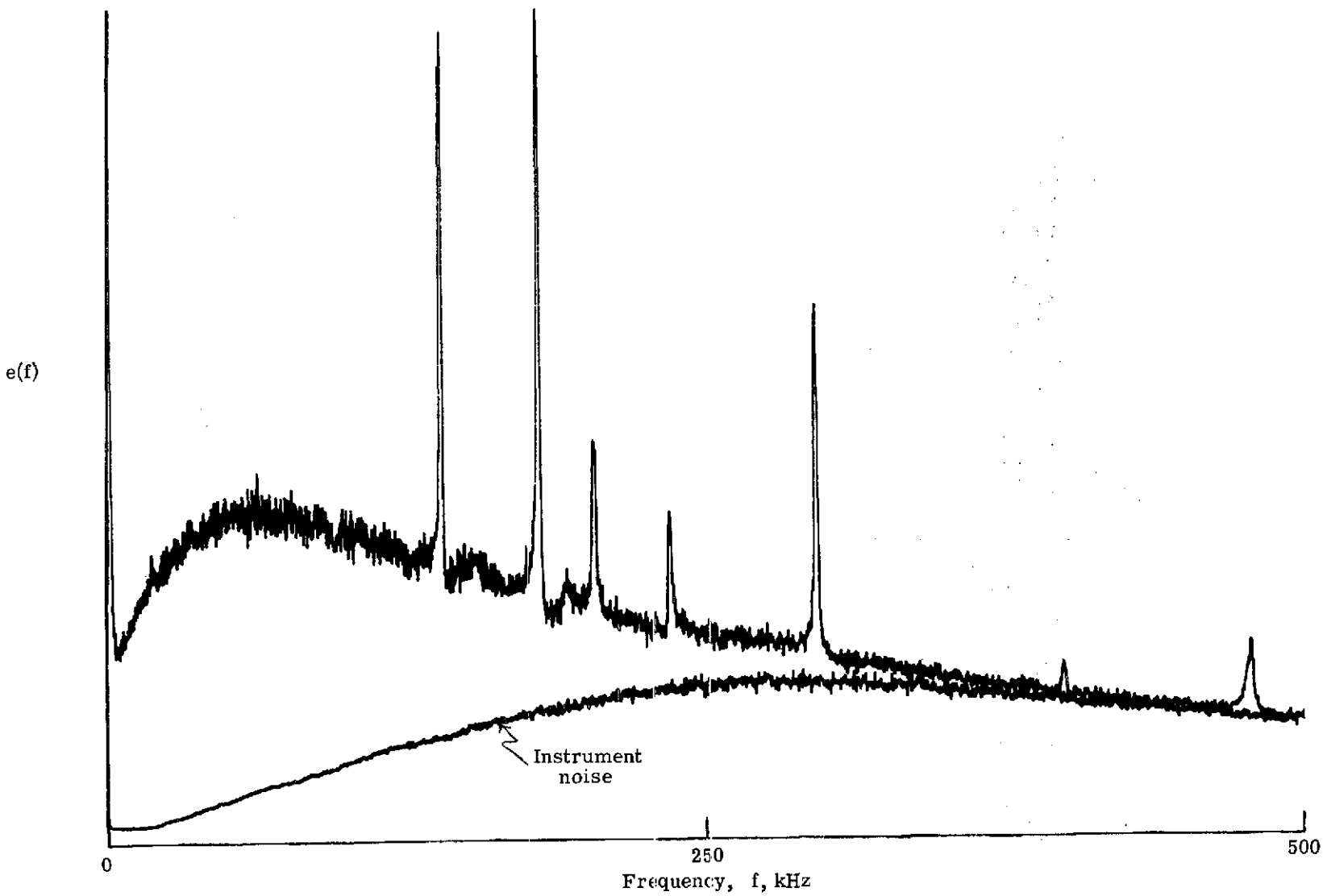

(a) Wire with strain-gage oscillations.

Figure 4.- Illustration of wire-strain-gage check.

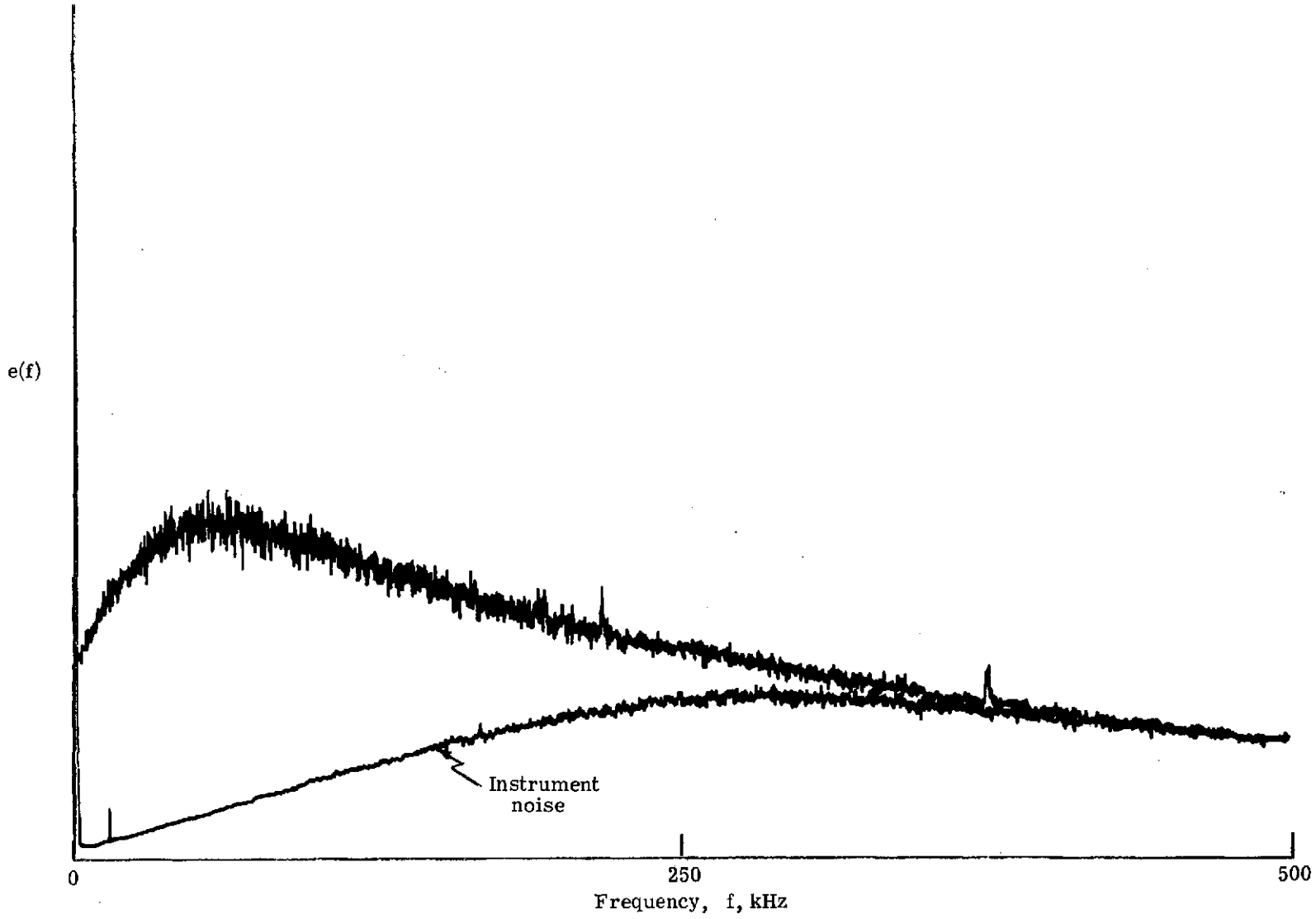

(b) Good wire.

Figure 4.- Concluded.

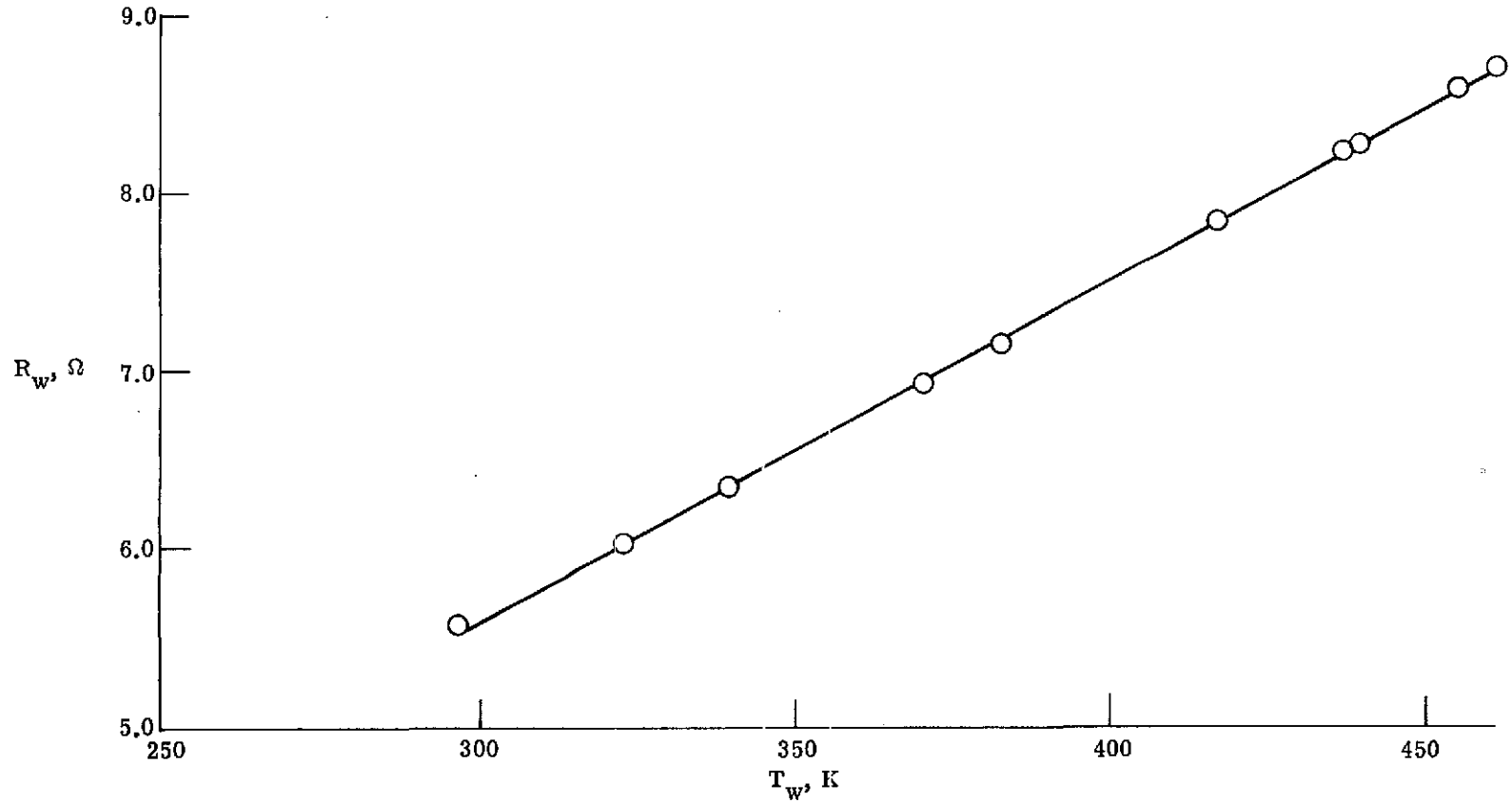

Figure 5.- Resistance-temperature calibration.

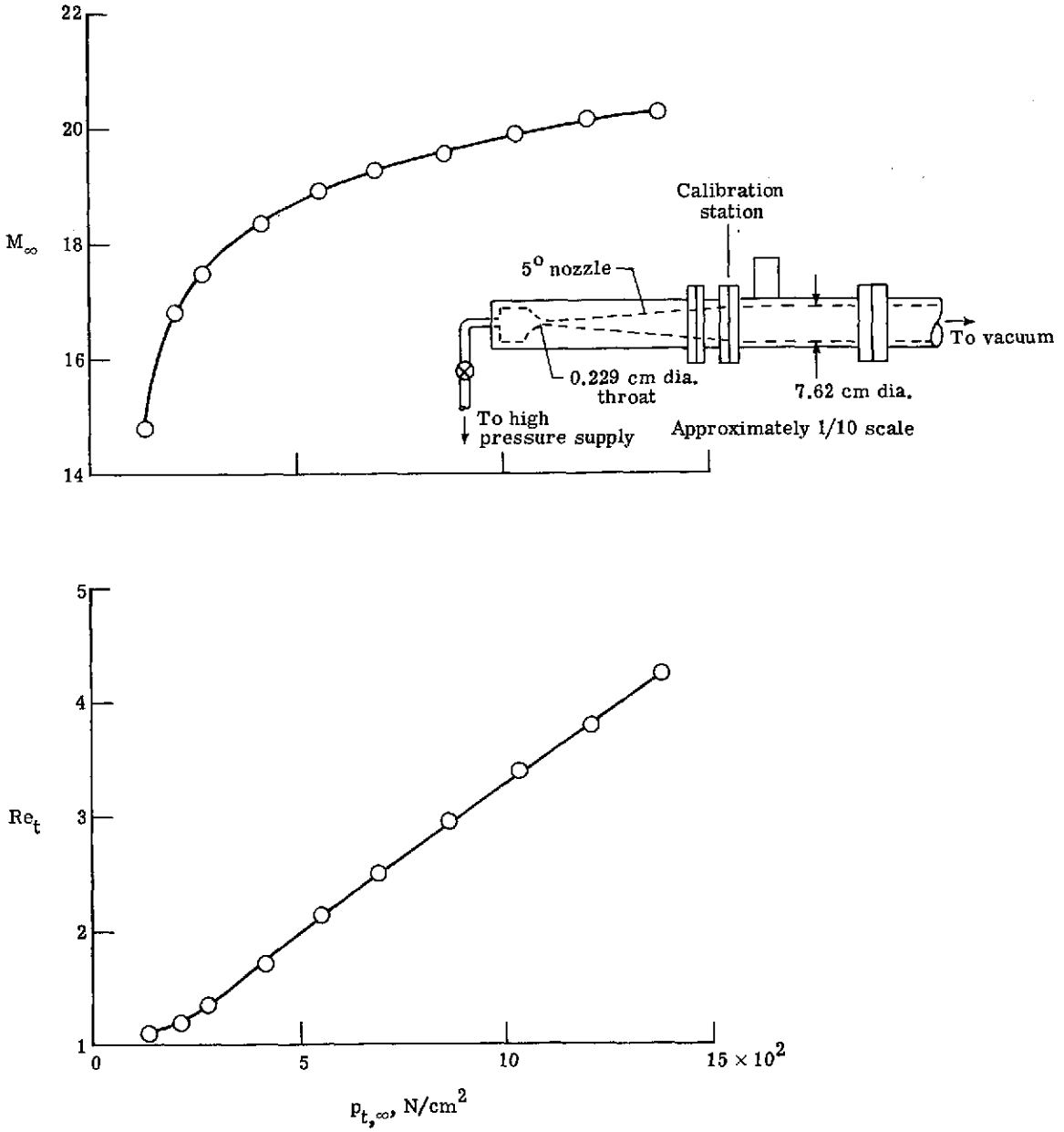

Figure 6.- The 7.62-cm nozzle calibration. $T_{t,\infty} = 305$ K. (Note: Maximum center-line Mach number gradient about 0.26 per cm.)

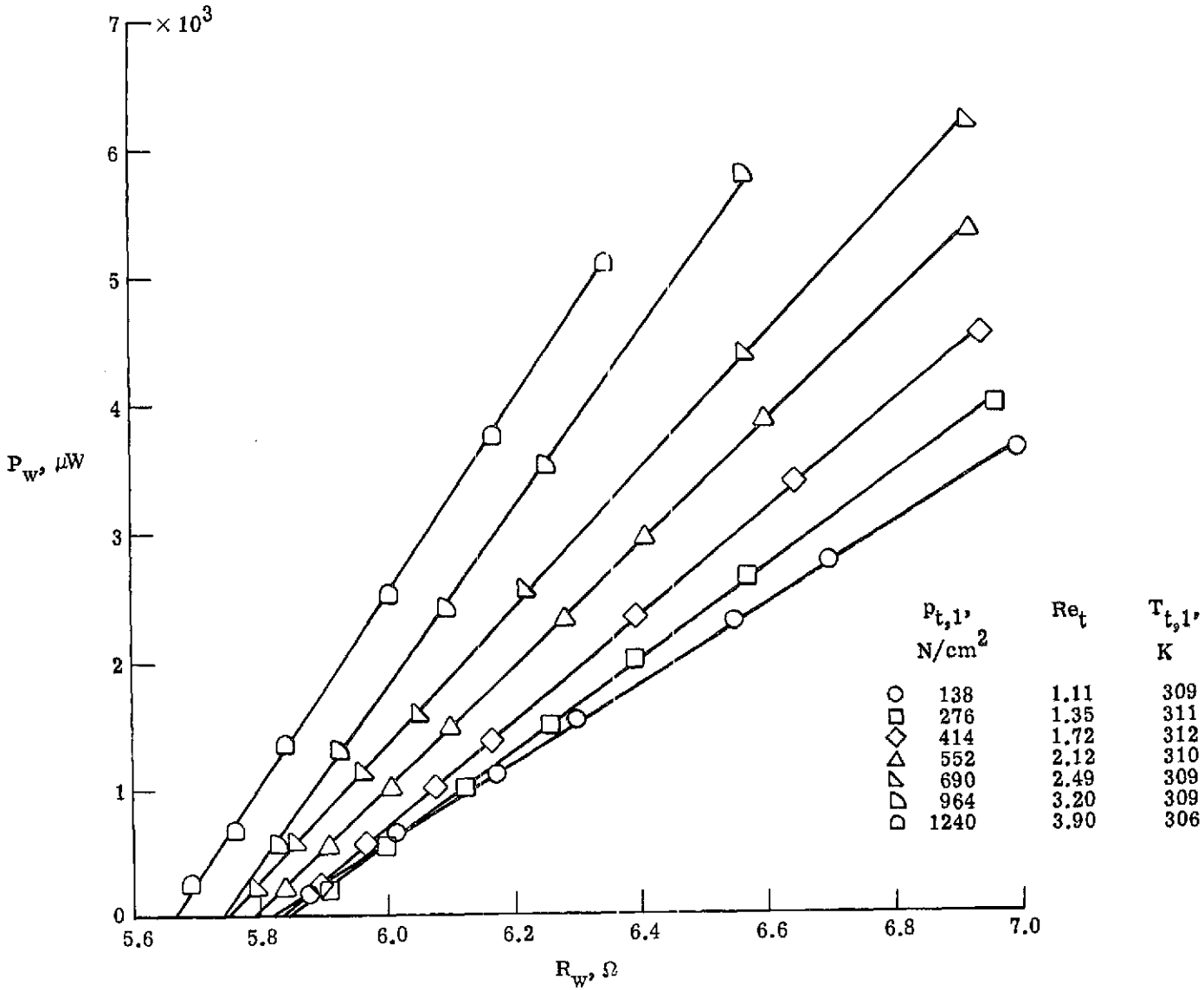

Figure 7.- Typical calibration data.

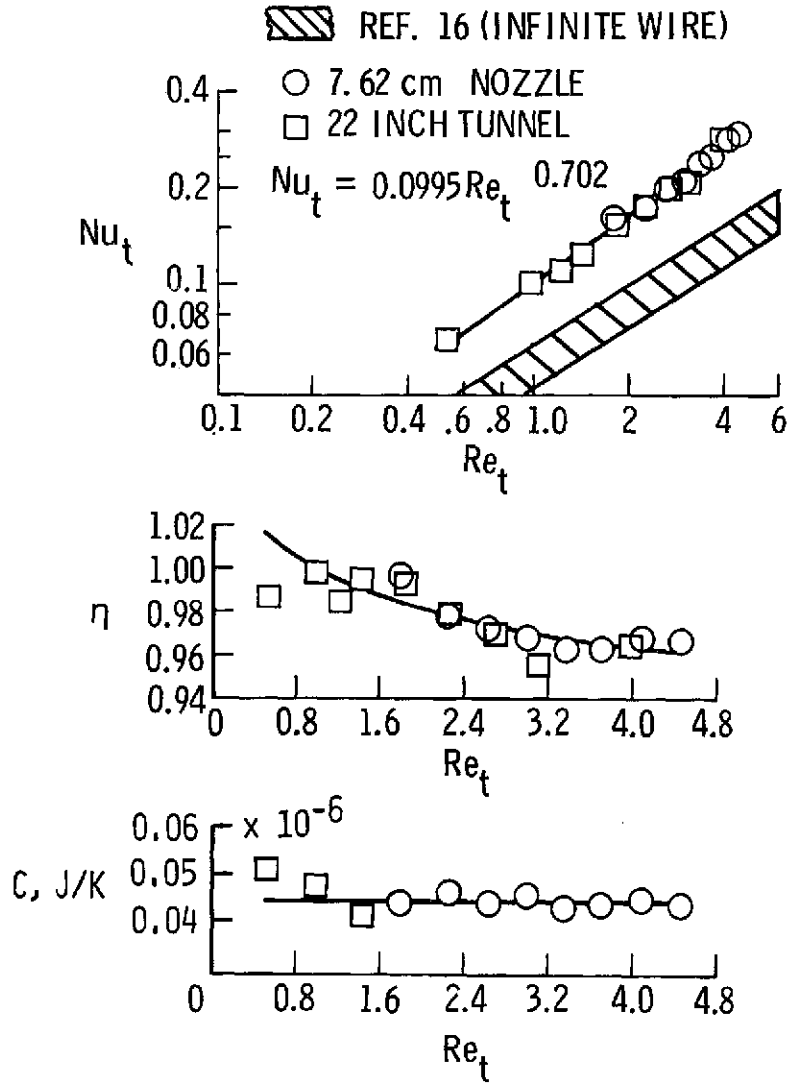

Figure 8.- Typical hot-wire calibration.

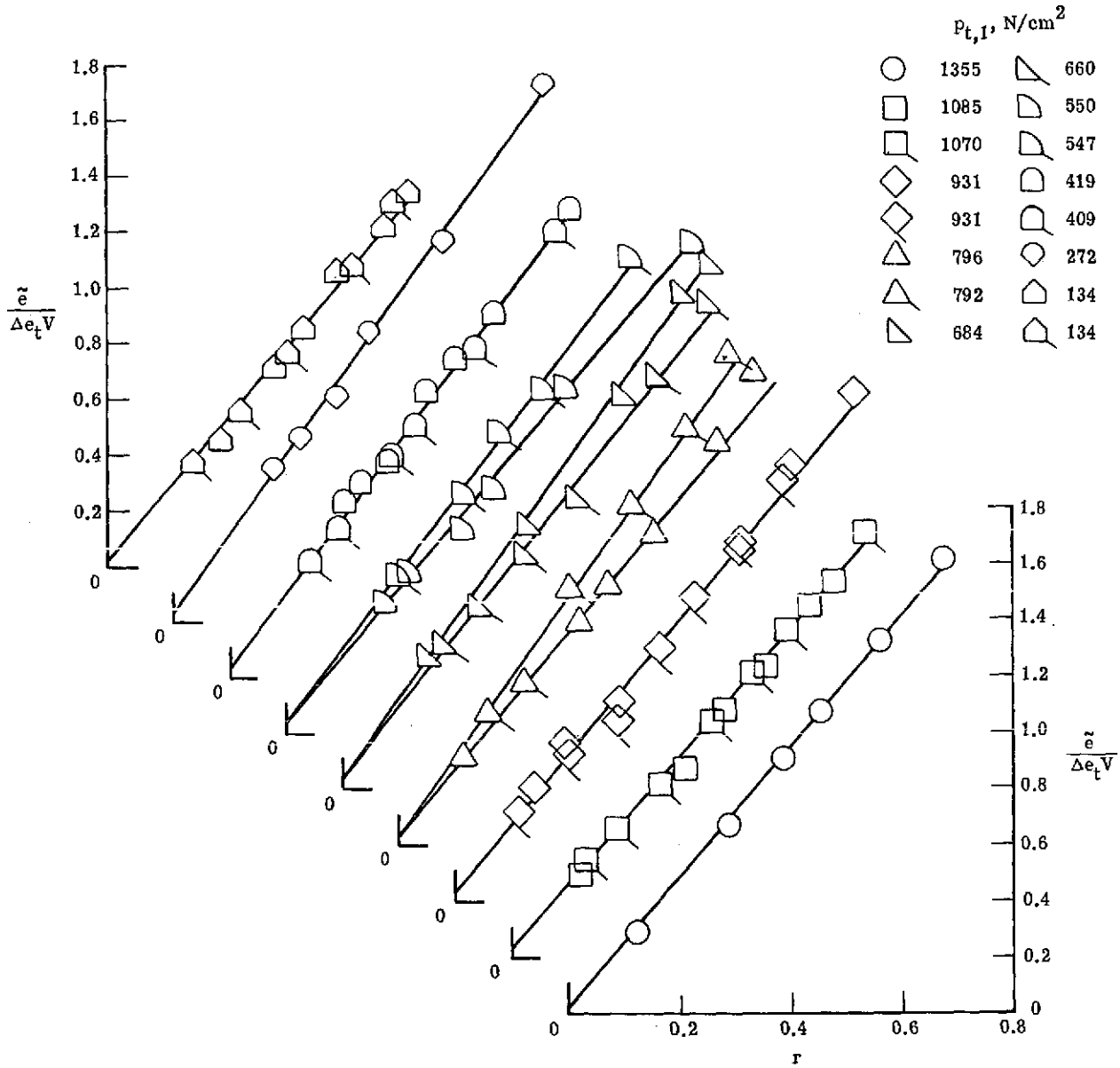

Figure 9.- Mode diagrams in the HRNHT.

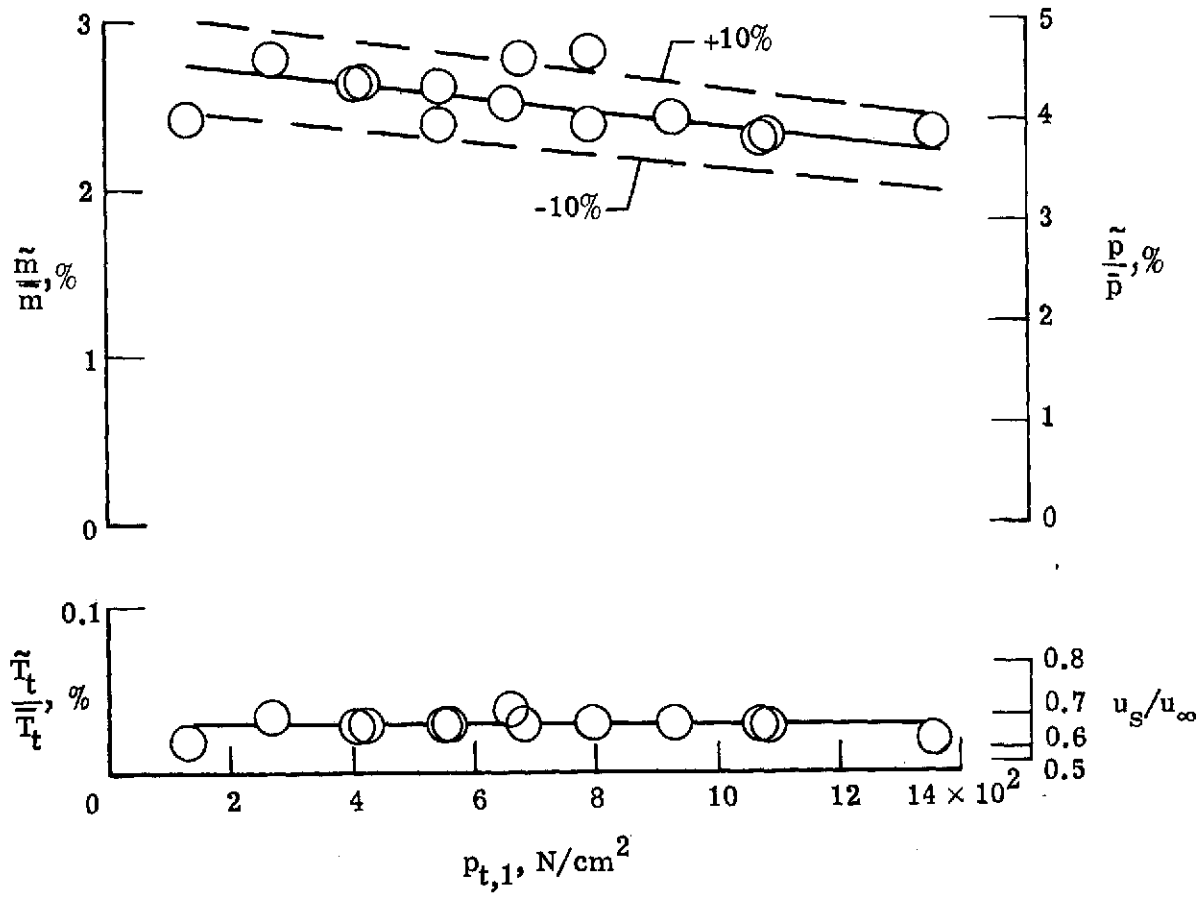

Figure 10.- Root-mean-square mass-flow and total-temperature fluctuations in the HRNHT.

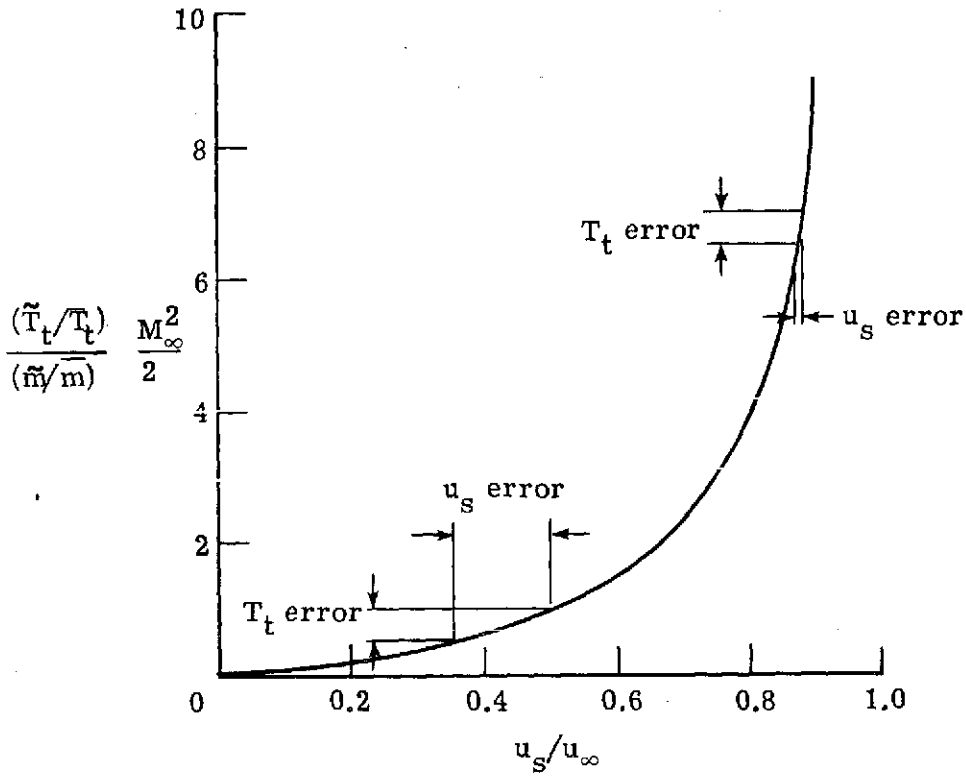

Figure 11.- Relation of source velocity to mass-flow and total-temperature fluctuation levels.

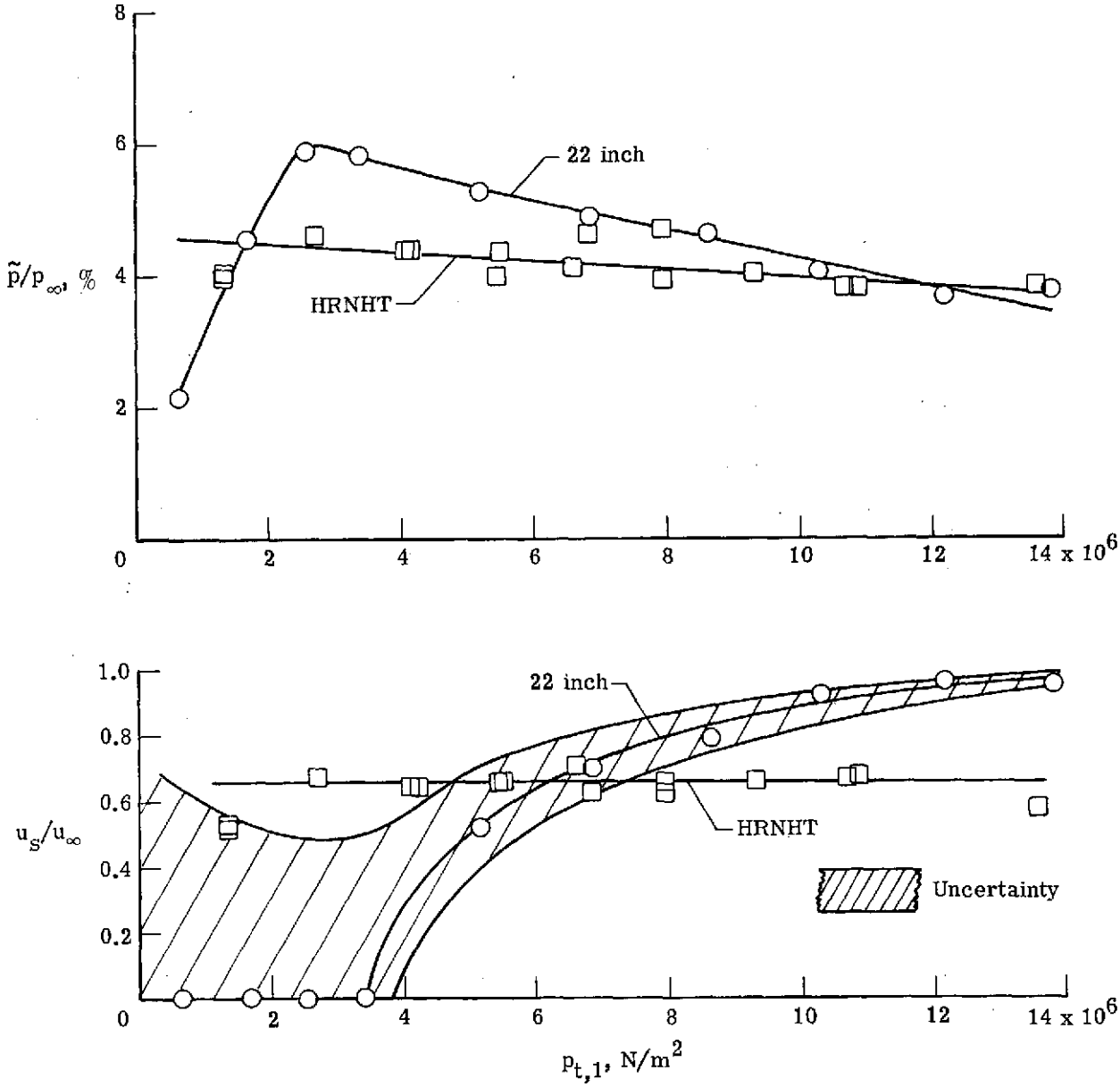

Figure 12.- Pressure-fluctuation levels and relative source velocities in the 22-inch hypersonic helium tunnel and the HRNHT.

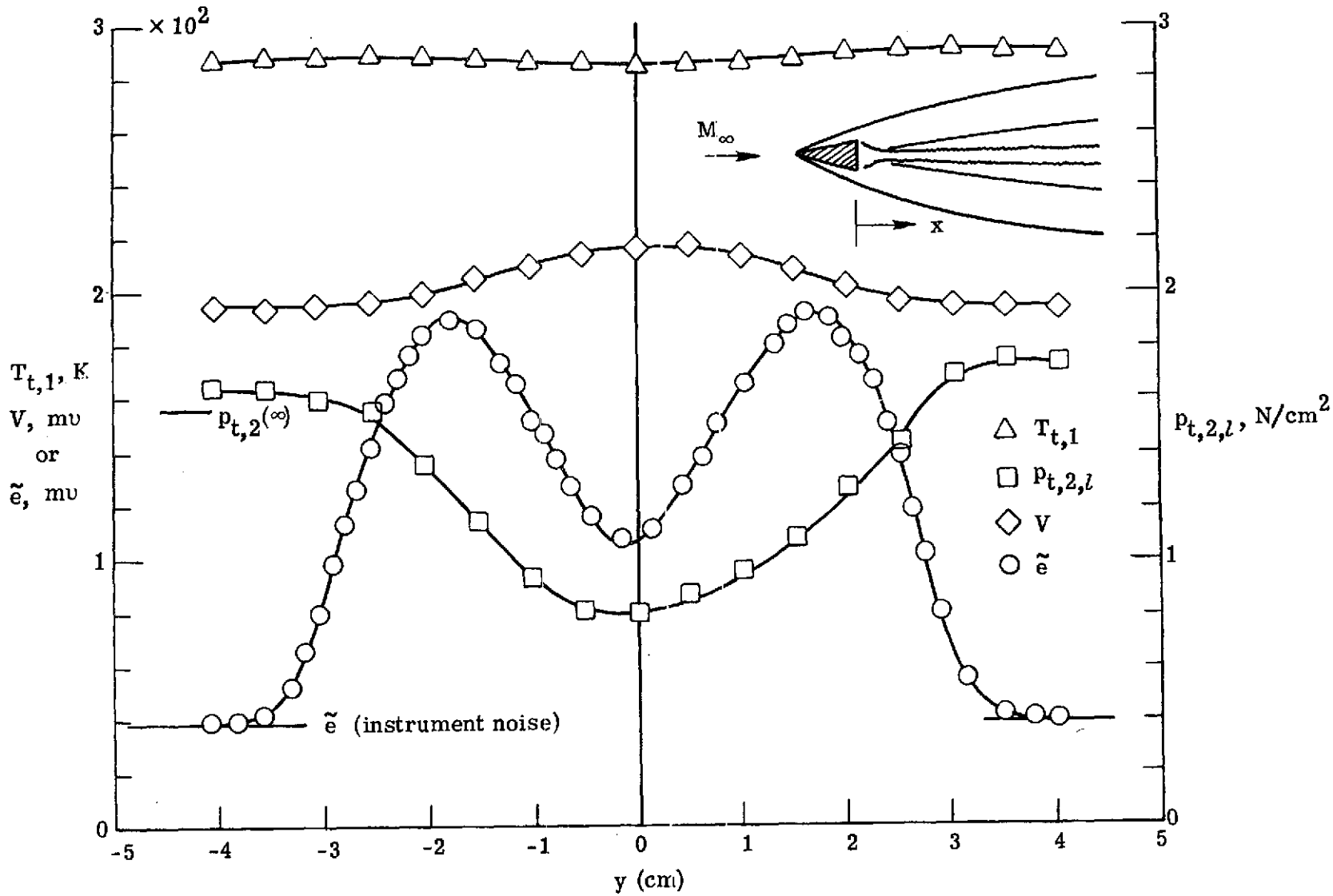

Figure 13.- Hot-wire, pitot tube, and total temperature probe survey of the wake of 15° half-angle wedge.

$M_\infty = 15.5$; $x/t = 68.3$; $I_w = 43$ mA; and $\frac{R_w - R_v}{R_v} \approx 0.35$.

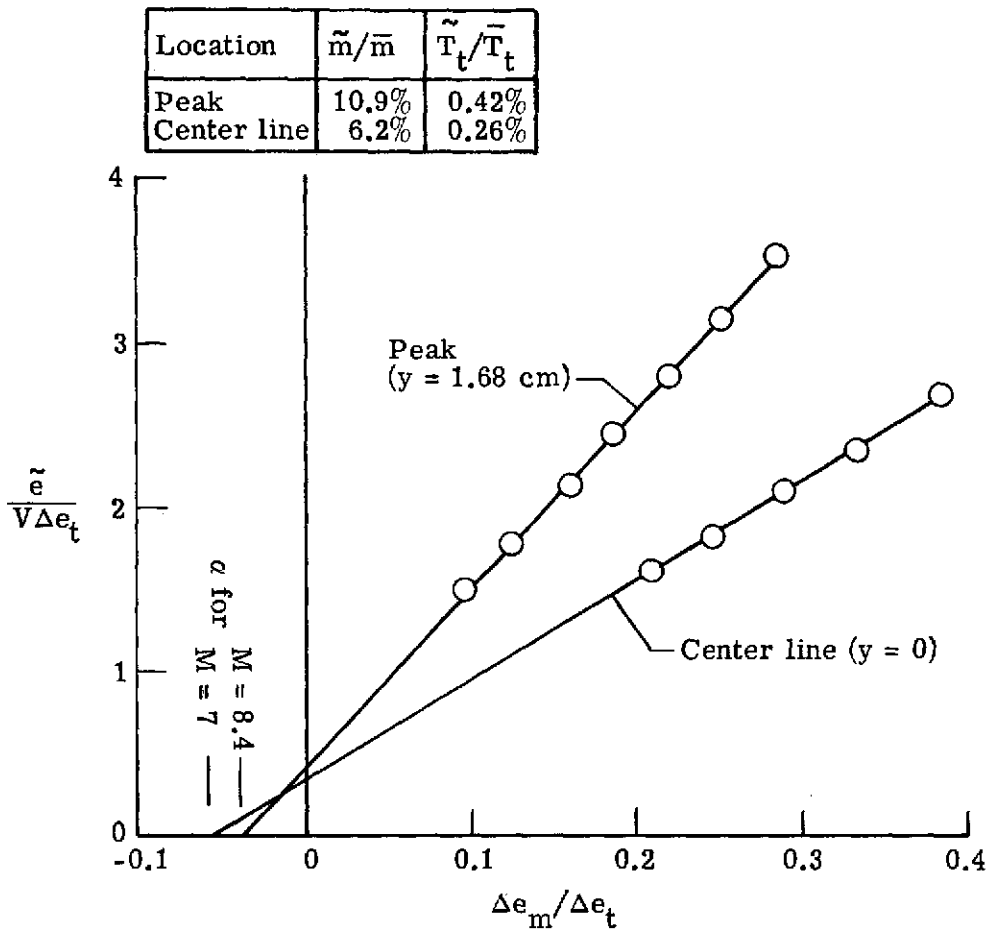

Figure 14.- Mode diagrams in wake of 15° half-angle wedge.

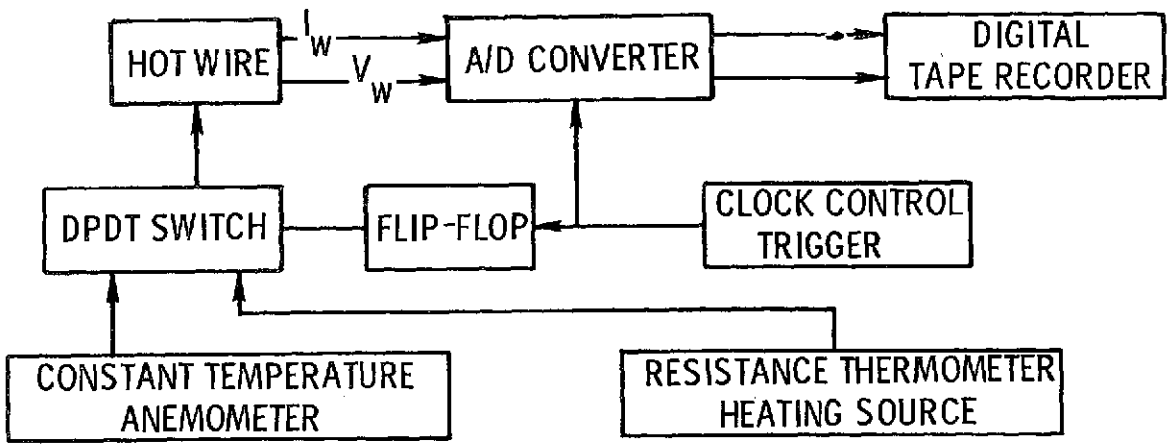

(a) Diagram of dual overheat instrumentation.

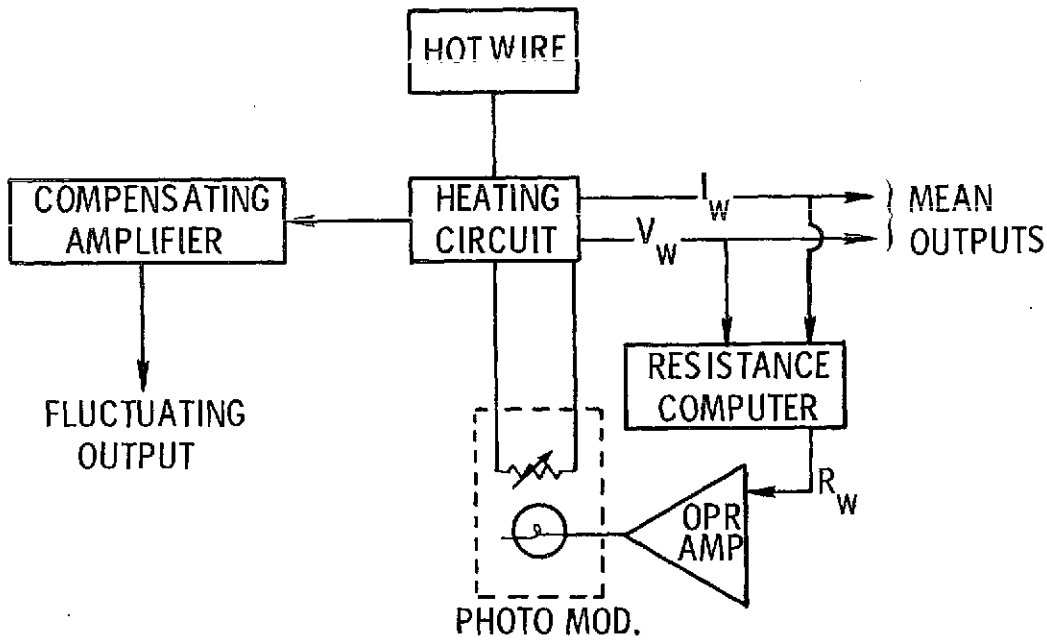

(b) Diagram of temperature controlled constant-current anemometer instrumentation.

Figure 15.- Diagrams of modified hot-wire instrumentation.

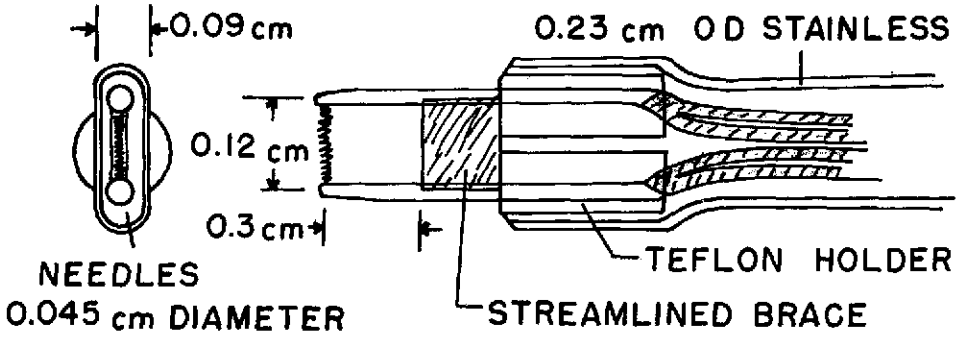

(a) Probe geometry.

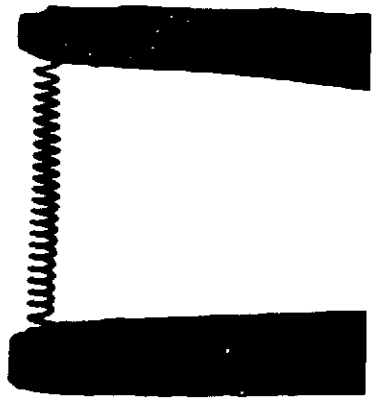

L-74-1073

(b) Photomicrograph of wire mounting.

Figure 16.- Hot-wire coil-probe construction.

A motion-picture film supplement L-1152 is available on loan. Requests will be filled in the order received. You will be notified of the approximate date scheduled.

The film (16 mm, 5 min, color, silent) shows steady level flight, progression of wing stall and directional divergence for the basic configuration, and directional divergence for the swept- and delta-wing configurations and the high basic and high delta configurations.

Requests for the film should be addressed to:

NASA Langley Research Center
Att: Photographic Branch, Mail Stop 171
Hampton, Va. 23665

CUT

Date_____

Please send, on loan, copy of film supplement L-1152 to TN D-7716.

_____
Name of organization

_____
Street number

_____
City and State Zip code

Attention: Mr._____

Title_____